COSMIC-2 Capabilities for Monitoring Ionospheric Scintillation

Dr. Paul Straus[1], Dr. Charles Carrano[2], Dr. Keith Groves[2], Dr. William McNeil[2], Dr. Sergey Sokolovskiy[3], Dr. Irina Zakharenkova[3], Dr. Qian Wu[4], Dr. Endawoke Yizengaw[1], Dr. Iurii Cherniak[3], Dr. John Braun[3], Doug Hunt[3], Teresa VanHove[3]

[1]The Aerospace Corporation

[2]Boston College

[3]University Consortium for Atmospheric Research

[4]High Altitude Observatory

12 September 2022

COSMIC-2 Scintillation Capabilities Overview

- COSMIC-2 is putting in place several new radio occultation (RO)-based capabilities for routinely monitoring equatorial ionospheric scintillation
- "All-Clear": specifies longitude regions in which UHF scintillation is <u>not</u> present
  - *Also applies to higher frequencies, but is overly conservative in such cases*
  - *Based on analysis of TGRS "low rate" (1Hz) observations of L1 SNR*
- Geolocation: determines locations of irregularity regions that cause scintillation
  - *Based on analysis of TGRS "high rate" (50Hz: GPS or 100Hz: GLONASS) L1 SNR & carrier phase data at ionospheric tangent altitudes (collected via POD antennae)*
  - *Two different algorithms have been validated by the COSMIC-2 Cal/Val effort*
  - *Boston College (BC) algorithm*
  - *UCAR algorithm*
- "Bubble Map": amalgamates the geolocation algorithm results into a single map to provide a global (equatorial latitudes) picture of ionospheric instability regions
  - *Can employ either BC or UCAR geolocation products*
  - *Various future augmentations possible, including incorporation of in-situ density data from the IVM sensor on COSMIC-2*

“All Clear” Algorithm Concept (1 of 2)

Originally developed with RO data from the C/NOFS mission

- All Clear infers the absence of ionospheric irregularities from the absence of scintillation observed by TGRS using a simple premise
  - *Regions most likely to be free of irregularities when scintillations are **not** observed are the same as those most likely to contain irregularities when scintillations are observed*
- Occulting ray path segments that would likely have strong irregularities if scintillation were present are considered irregularity-free if scintillation is not observed
- An ad hoc (“PCA Index”) model developed by BC describes irregularity probability as a function of apex altitude and climatological electron density

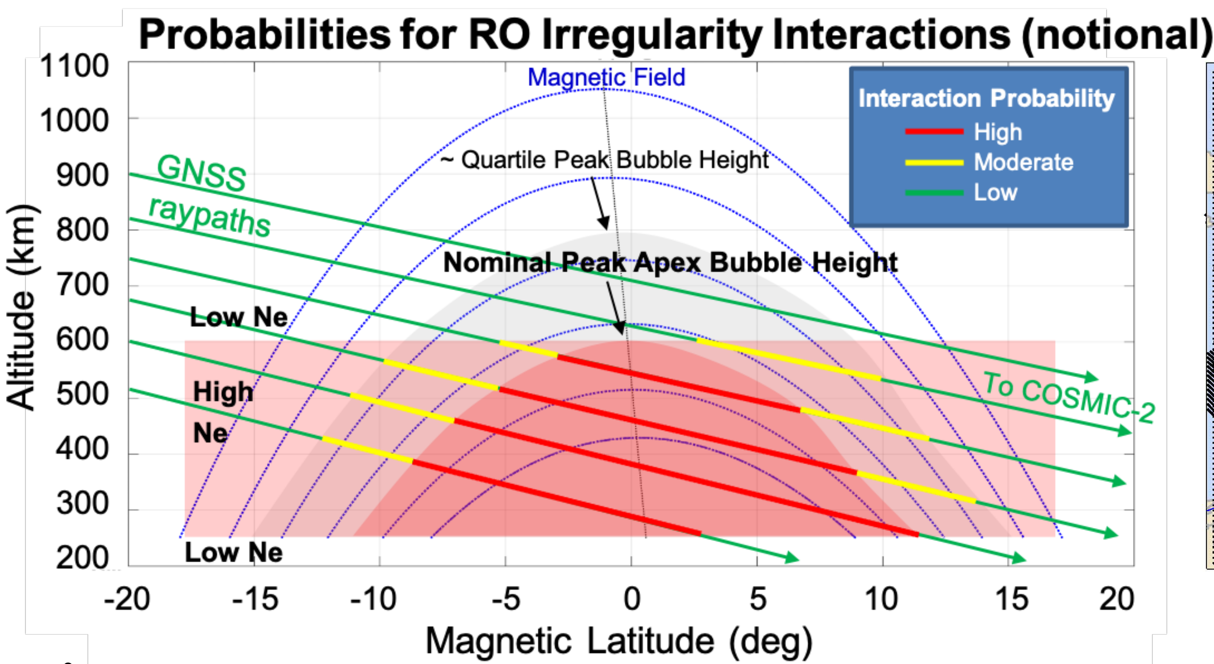

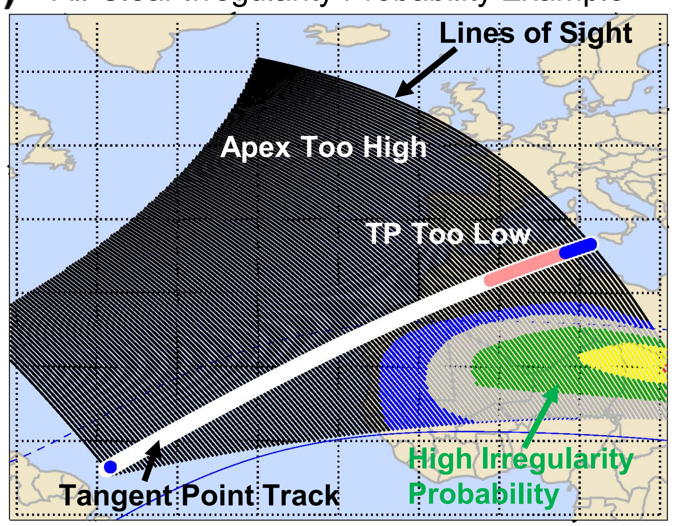

“All Clear” Algorithm Concept (2 of 2)

- Presence of scintillation is assessed via the 31s pseudo-S4 index (SNR data contaminated by RFI is excluded from the analysis)
- For each epoch, a “PCA Index” map is generated, showing the regions most likely to be devoid of irregularities based on all occultations observed by the full COSMIC-2 constellation
- All Clear maps are generated by extending regions in latitude to model the expansion of irregularities along magnetic field lines
- Green regions: >95% chance of no scintillation
- Yellow regions: >75% chance of no scintillation
- Gray regions: indeterminate (no coverage or scintillation observed)

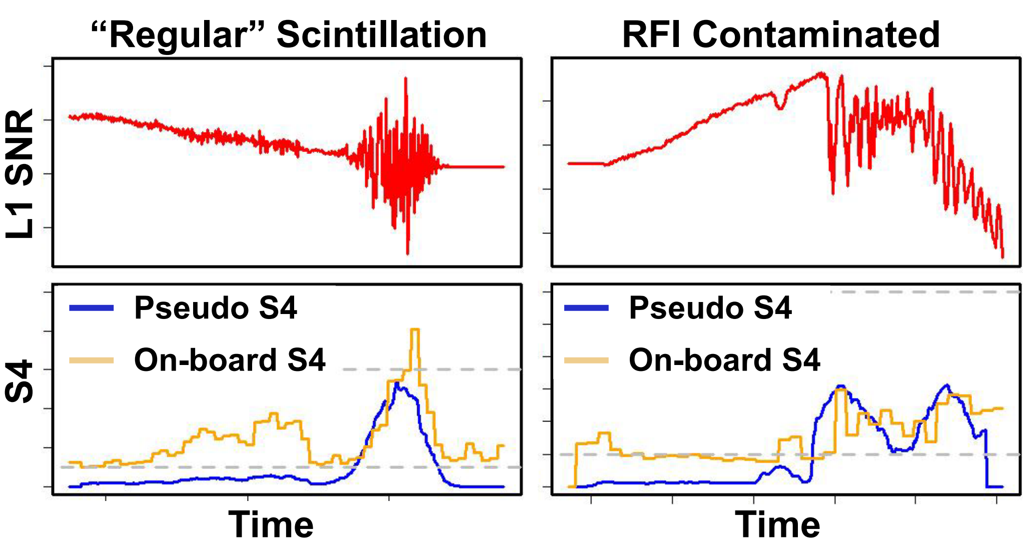

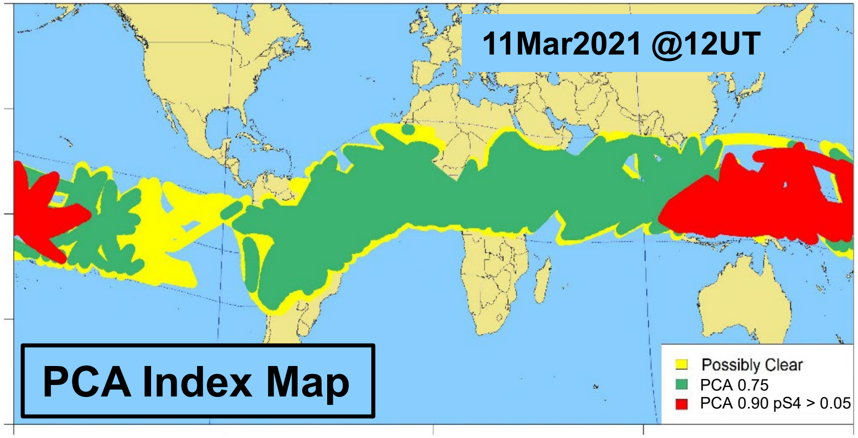

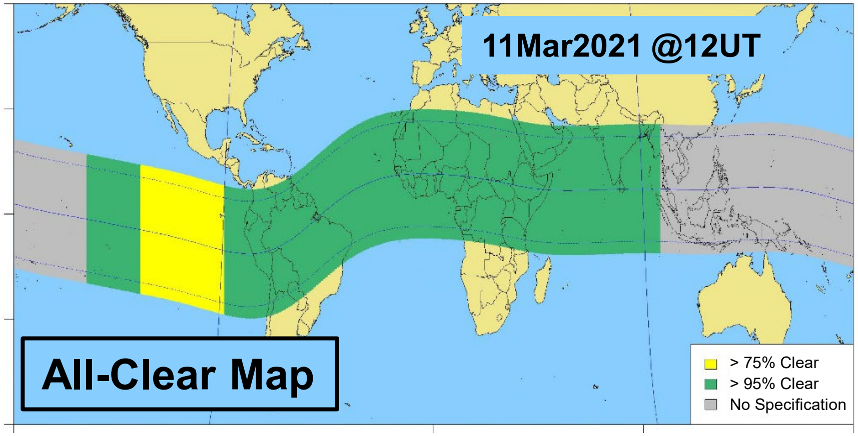

All Clear Validation

<u>Validation Time Periods</u>
01 Sep - 15 Oct 2020
06 - 31 Mar 2021

- All Clear specifications were compared to ground-based scintillation observations from
  - *(1) VHF SATCOM receivers (S4)*
  - *(2) S4 inferred from GNSS receiver Rate-of-TEC-Index (ROTI) – analysis determined that ROTI was an adequate proxy for S4 during pre-midnight local times*
- Ground-based GNSS receiver scintillation measurements could not be used for validation because of the weak L-band scintillation under these solar minimum conditions

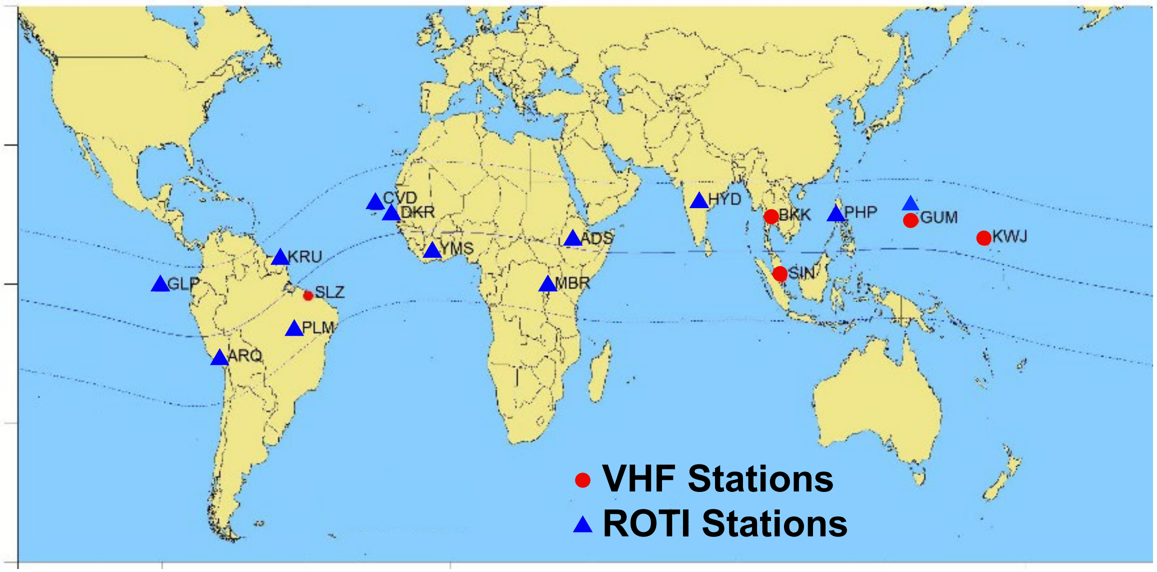

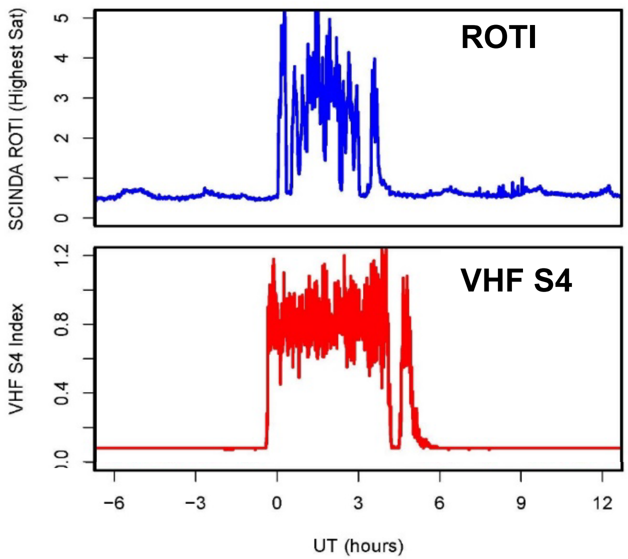

"Green specification" performance was determined to be accurate 97.5% of the time

TGRS Ionospheric HR Data Enables Geolocation

- TGRS simultaneously collects “tracks” of GNSS satellite observations (GPS & GLONASS) made via POD antennae
  - *~16 channels of GPS*
  - *~9 channels of GLONASS*
- Tracks are comprised of occultation & arc portions (below/above 0° elevation)
- Every track provides
  - *L1 & L2 SNRs every 1s*
  - *On-board S4 every 10s*

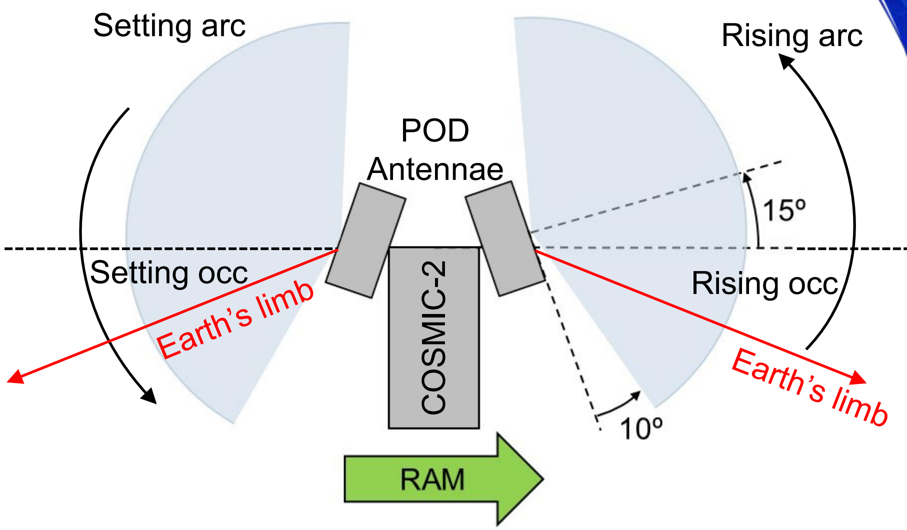

- For each rising or setting occultation TGRS analyzes the on-board S4 profile
  - *If scintillation is observed and certain threshold criteria are met, TGRS sends down high rate (HR) amplitude & phase data for the entire occultation*
- Total HR data volume is limited by TGRS’ data transmission capability
  - *HR data generation is shut down if an orbital (~95 min) volume limit is exceeded*
  - *This can limit the amount of TGRS HR scintillation data available for operational use*

Boston College (BC) Geolocation Algorithm

- Irregularities are geolocated via back-propagation in the time domain, with Fresnel frequency as the independent variable to be measured
- The Rino scintillation model (1979), generalized to RO geometry, is used to relate Fresnel frequency to Fresnel scale, and then to distance along the ray-path to the irregularity region.

$$U_s(t) = F^{-1}\left\{\exp\left[-\tfrac{1}{2}i(2\pi f / f_F)^2\right]F\left[U_{RX}(t)\right](f)\right\}$$

1. Back-propagate complex signal in 10-sec segments to measure Fresnel frequency of the scattering.

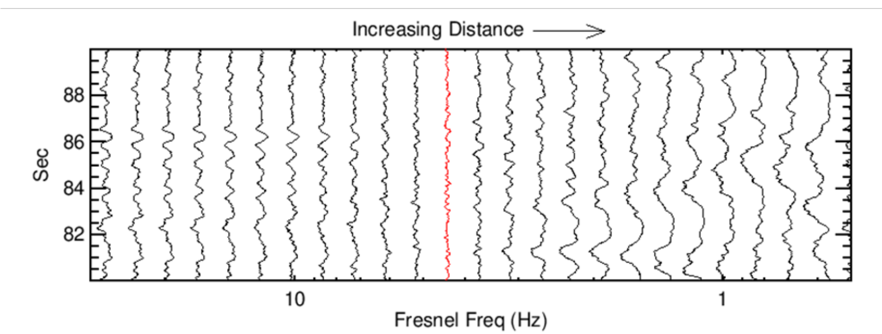

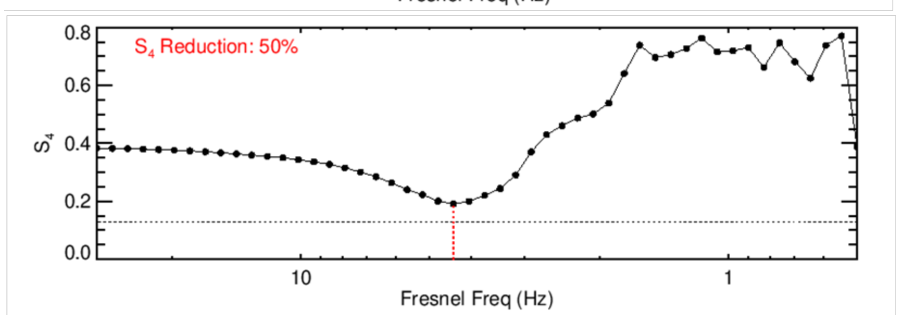

2. Geometric model provides Fresnel frequency vs distance. Intersection with measurement gives distance to irregularities.

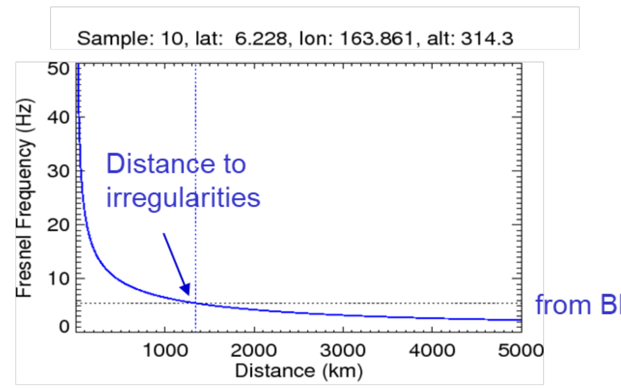

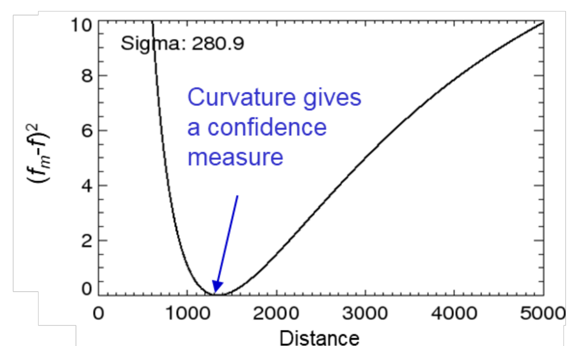

Mapping Fresnel Frequency to Irregularity Location

BC algorithm

- Scan velocity is proportional to the distance (d_s) from the irregularities

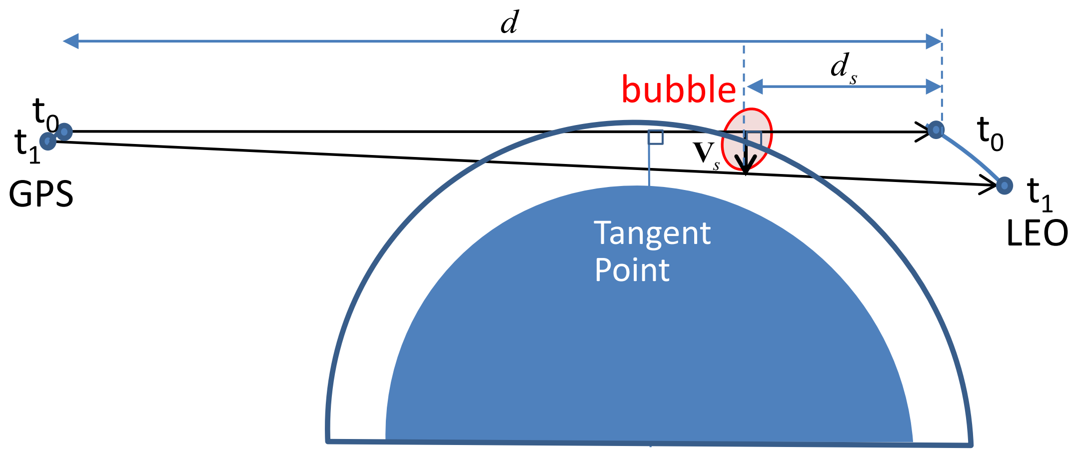

- For anisotropic field-aligned irregularities we must use an effective scan velocity, V_{eff}
- Effective scan velocity: $V_{eff}(d_s) = \left[\dfrac{CV_{sx}^2 - BV_{sx}V_{sy} + AV_{sy}^2}{AC - B^2/4} \right]^{1/2}$

V_{sx}, V_{sy} are components of V_s in plane $\perp$ to ray-path

- Fresnel frequency: $f_F(d_s) = V_{eff} / \rho_F$
- Fresnel scale: $\rho_F = \sqrt{\dfrac{d_R}{k}}, \quad d_R = \dfrac{(d - d_s)d_s}{d}$

Once $f_F(d_s)$ has been measured, this purely geometric model can be inverted to find d_s

UCAR Geolocation Algorithm

- Based on 2001GL013398, 2002 algorithm
- Numerically solves 2D Kirchhoff equation using TGRS observed amplitude/phase using phase screen approximation

$$u(\vec{r}) = \sqrt{\frac{k}{2\pi}} \int A(\vec{r}')\, cos\varphi_{rr'} \frac{\exp[ikS(\vec{r}') - ik|\vec{r} - \vec{r}'| + i\pi/4]}{\sqrt{|\vec{r} - \vec{r}'|}} d\vec{r}'$$

- Corrections for receiver motion & wave front curvature are applied
- Irregularities are geolocated via back-propagation (BP) at the location of the minimum of the back-propagated signal amplitude variance
- Because BP plane orientation depends on magnetic field (MF) orientation at the irregularity location (initially unknown), an iterative process is employed to search for the solution

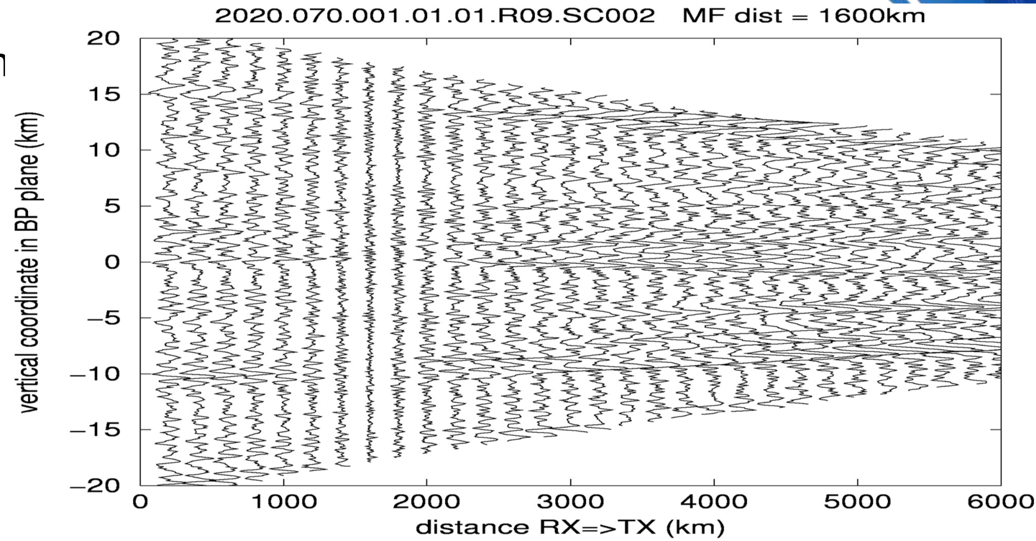

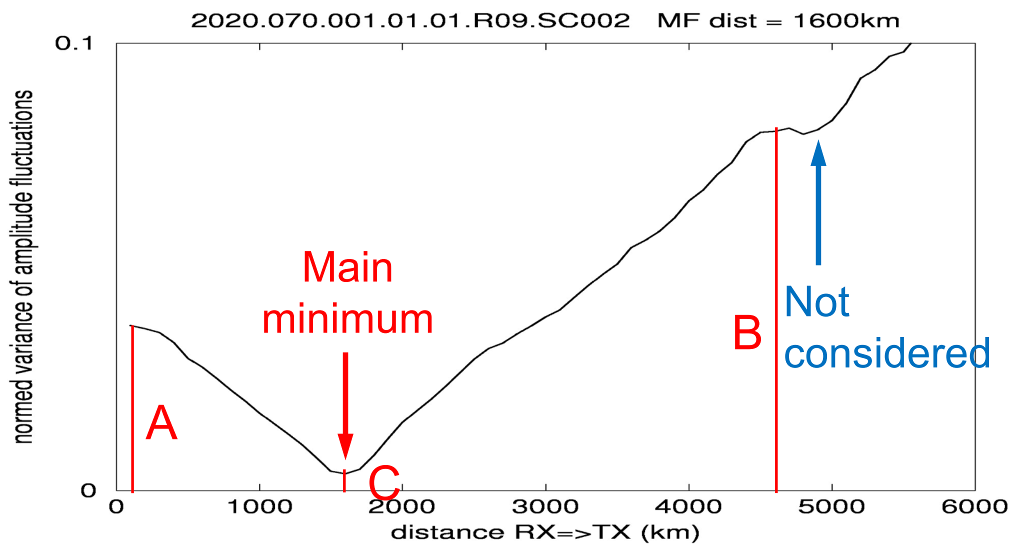

Major Differences Between BC & UCAR Algorithms

BC Algorithm

- Back-propagation used to determine Fresnel frequency of propagation
- High-pass filtering of raw phase data
- Entrance criteria: S4>0.13
- Success criteria: S4 reduced by >10%
- Magnetic field handled via effective scan velocity & Fresnel scale mapping to distance (no iteration needed)
- Irregularity aspect ratio 1:50
- No restriction on orientation of ray path relative to magnetic field

UCAR Algorithm

- Back-propagation used to determine distance to irregularities directly
- Based on UCAR excess phase
- Entrance criteria: σ_ϕ>0.33 rad
- Success criteria: Normed amplitude variance decreases by factor >1.2
- Magnetic field handled by iterative adjustment of BP plane
- Irregularity aspect ratio infinite
- Angle between ray path & magnetic field must be <75°

Validation via NASA GOLD Comparisons

- GOLD 135.6 nm O^+ recombination imagery scales with square of ionospheric density
- Ionospheric depletions ("bubbles") are associated with instability/irregularity regions
- GOLD bubble locations/widths were initially identified by UCAR analysis, then manually sanity checked by Cal/Val team
  - *GOLD bubbles identified by the process were validated vs. ground-based VHF scintillation data (Sao Luis, Brazil): 100% agreement wrt pre-midnight scintillation*

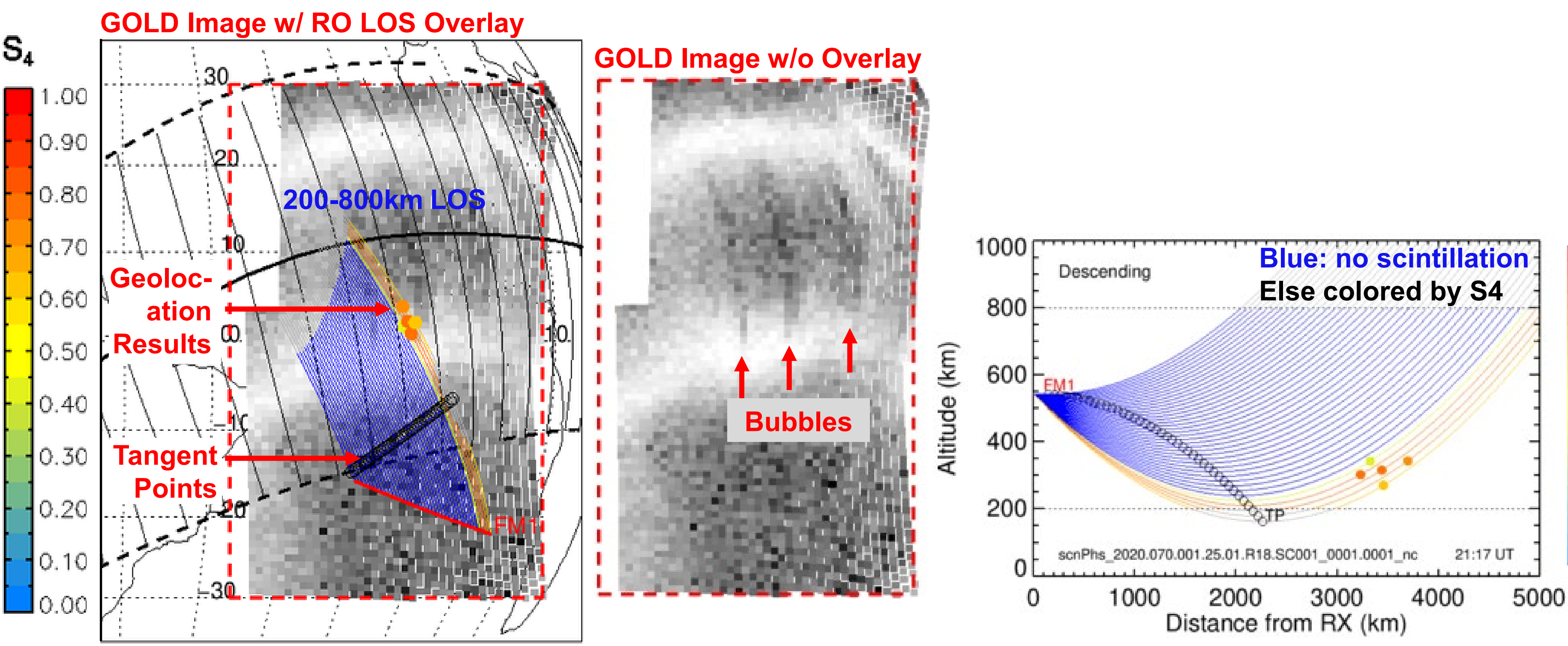

Multiple Bubbles Detected in Single Occultations

- Various occultation geometries result in potential detection of multiple bubble regions
- However, TGRS may not detect all bubbles – just those intersected by the RO ray-paths at F-region altitudes (assuming that TGRS downlinks HR data for the occultations)

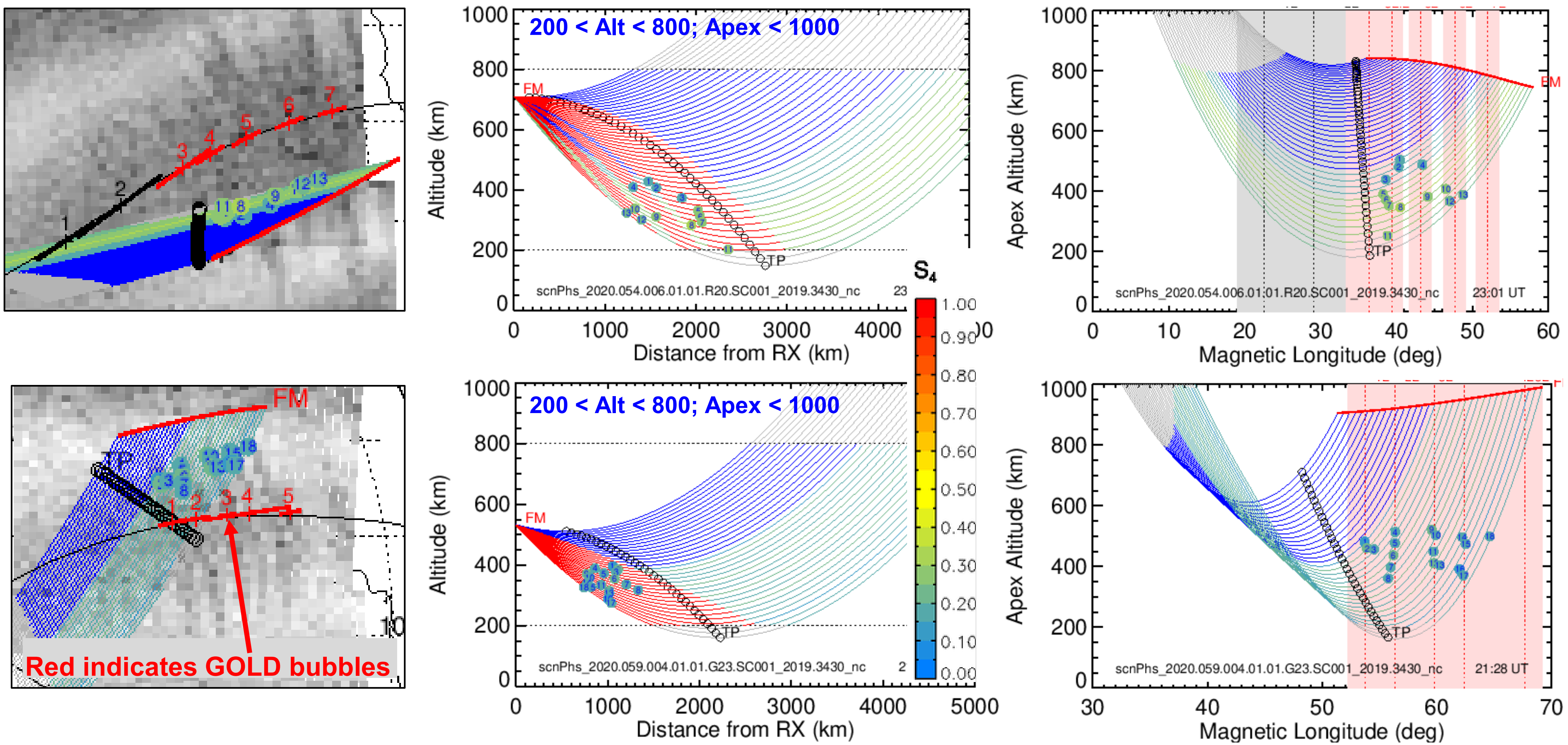

GOLD Validation Results

- Both algorithms assessed for 15 Feb-15 April 2020 time period
- Both algorithms performed well (BC slightly better)
  - *BC: 90% of geolocations within 1° of GOLD*
  - *UCAR: 90% of geolocation within 2° of GOLD*
- Outliers (>5° differences) were carefully evaluated
  - *Most of these cases involved lower quality GOLD imagery near the geolocations (bubbles may have been present, but not with certainty)*

	BC	UCAR
Error	% Cases	% Cases
0°	77	70
<1°	90	84
<2°	95	90
<5°	98	98

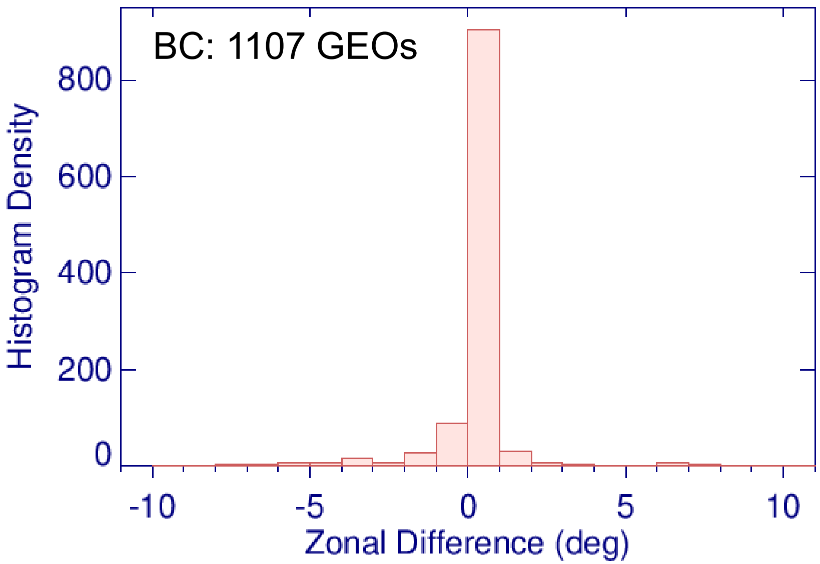

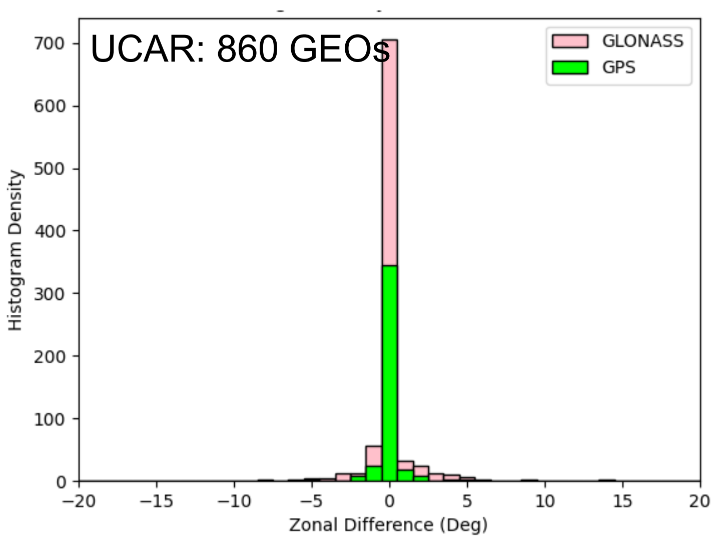

BC Geolocation Validation Outside of S. America

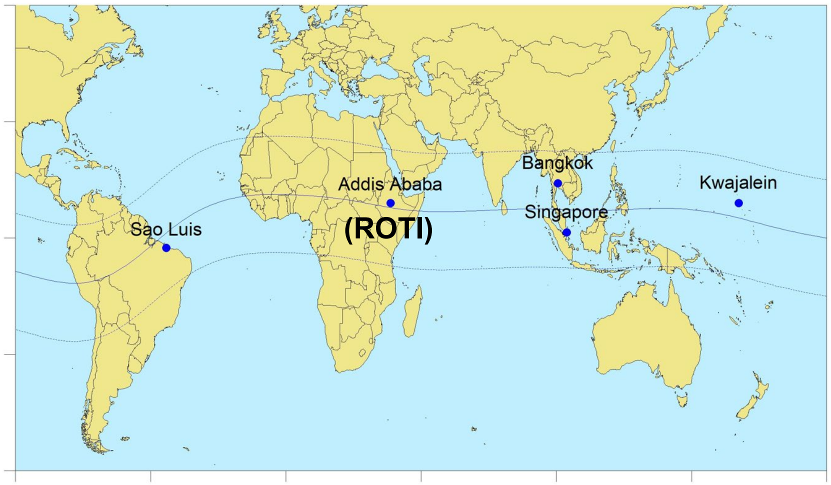

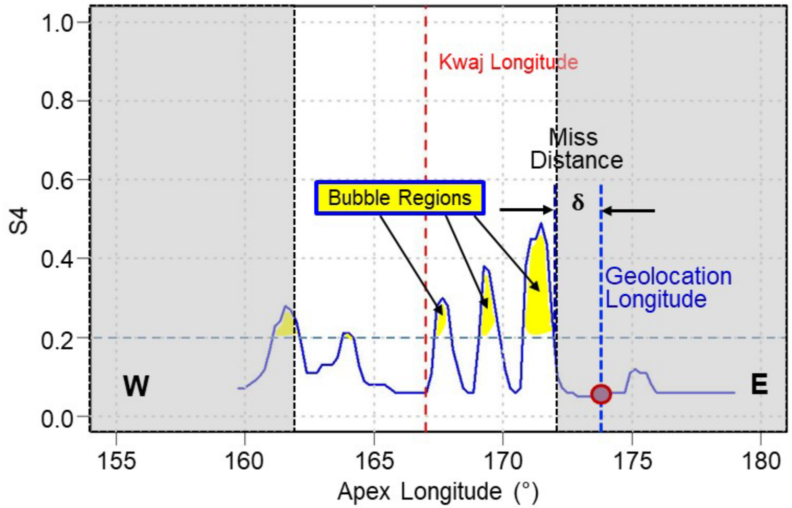

- Ground sensor for geolocation accuracy evaluation
  - *Receivers tracking VHF geostationary satellite signals*
  - *GPS receiver ROTI data (Addis Ababa station only)*
- Analysis assumes bubble structures observed by ground are "frozen in" and drift at 75 m/s
  - *Bubbles identified relative to 0.2 S4 sensor noise floor & projected out for 2 hours (5° longitude)*
  - *Pre-midnight events only*
- Geolocation accuracy for 4 non-S. American stations similar to GOLD analysis (90/96% are within 1°/2° longitude)

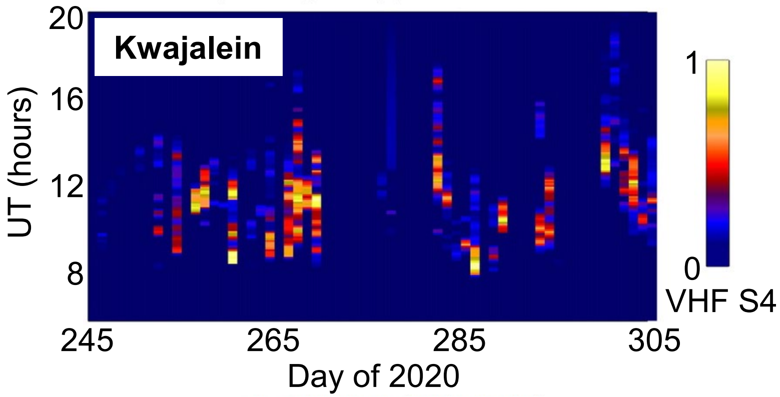

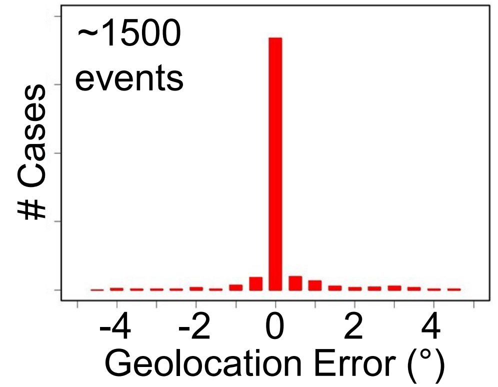

Inter-Comparison of BC & UCAR Algorithms

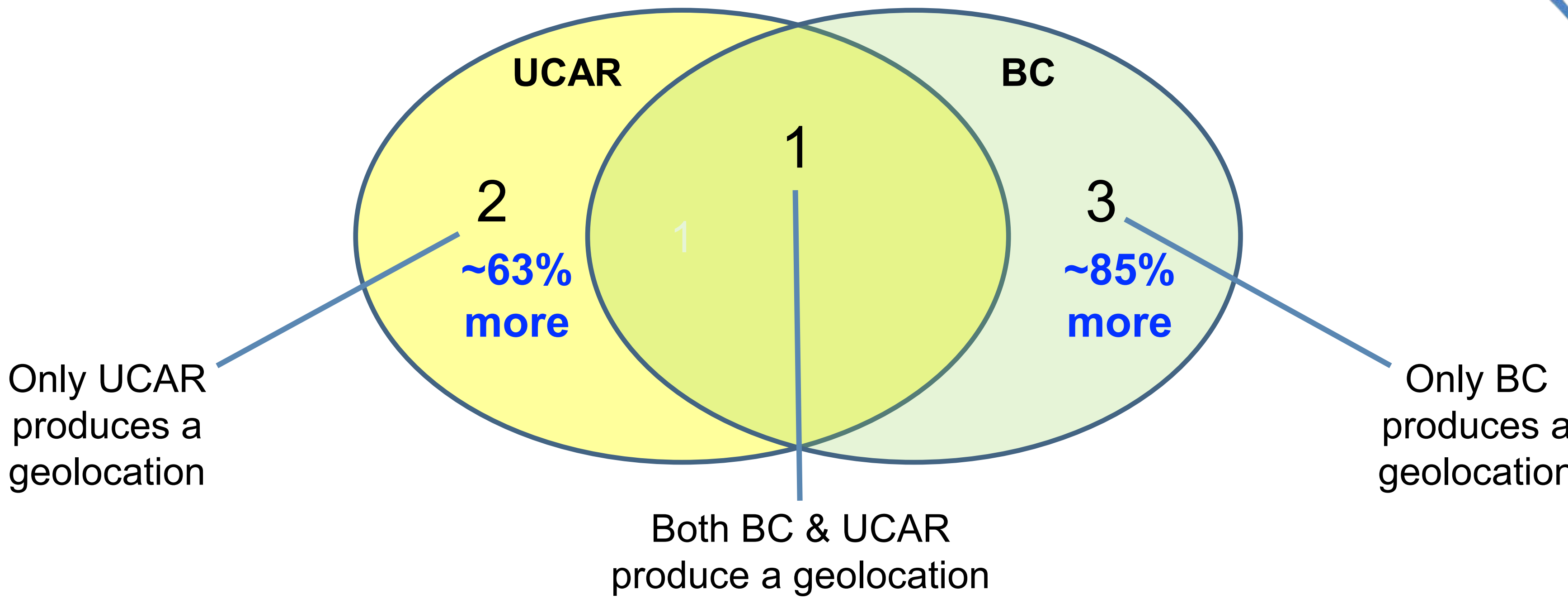

- UCAR compared their “common” geolocations with BC’s and found generally good agreement
- A small number of outlier cases (>5° differences) were carefully investigated
  - *No clear indications of algorithm flaws were identified*
  - *In many cases both algorithms may be right (sensitivity to different bubbles along LOS)*
  - *Ideas for improving the UCAR algorithm have arisen from these investigations*

The "Bubble Map"

Geolocation amalgamation

- Algorithm provides a coherent picture of low latitude irregularity region locations based on combining all available COSMIC-2 geolocations
- This analysis was performed using the BC algorithm geolocations
- It will be applied to UCAR geolocations in the future
- Current bubble "coloring" is based on TGRS S4 observations in the RO limb-viewing geometry
  - *Translation to the space-to-ground geometry is planned for the future*

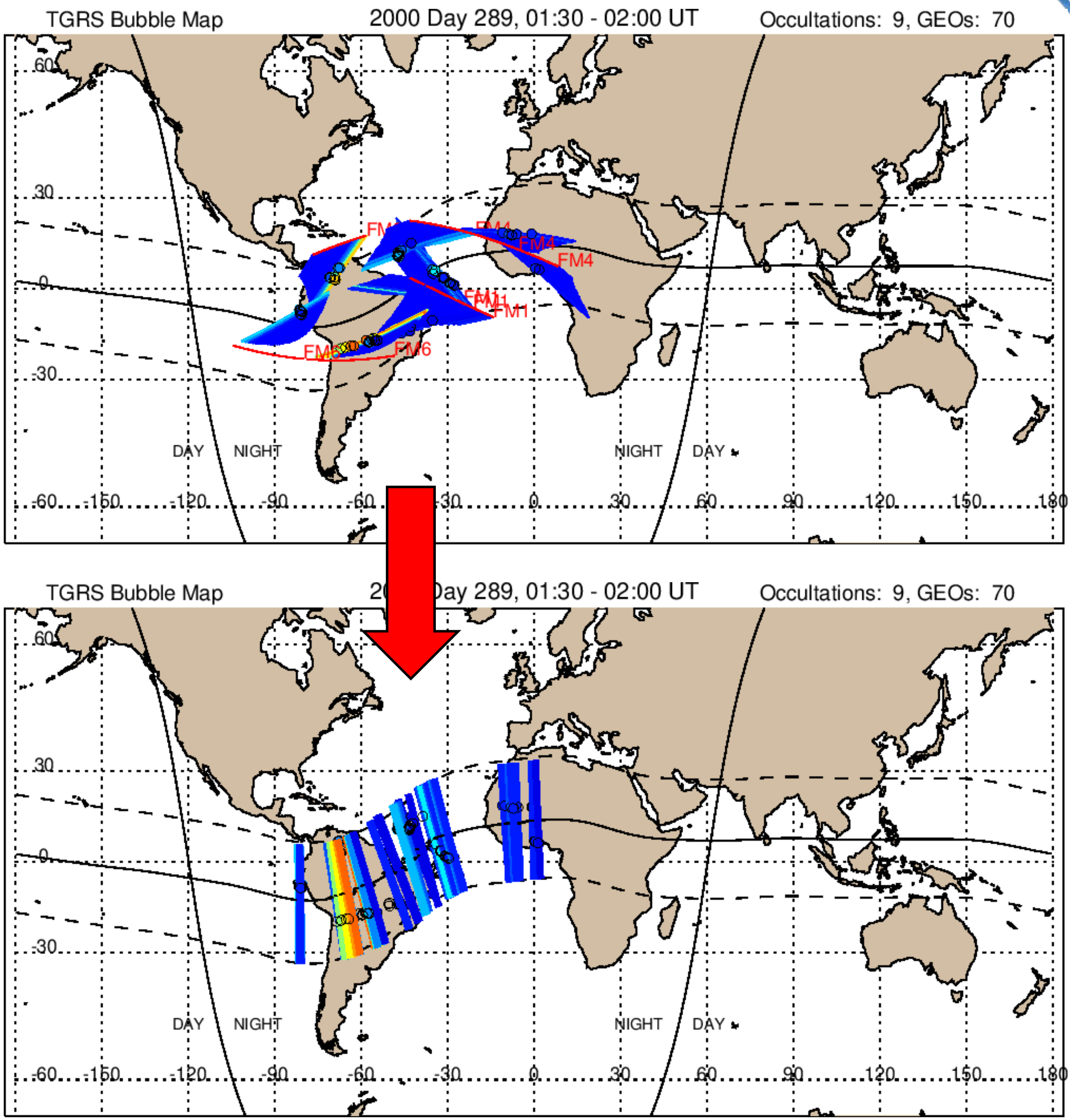

Bubble Persistence & Propagation in the Maps

- Once a bubble is detected, we know that it can persist, typically for a few hours
- Since TGRS/COSMIC-2 may not detect all bubbles, it may or may not re-sample persistent bubbles
- To improve Bubble Map "coverage", detected bubbles are propagated in the map for a specified duration (e.g. 60/90/120 minutes)
- Old bubbles are propagated to the valid time of the current map using a climatological zonal irregularity drift model
- Statistical analysis reveals that bubble persistence wouldn't be necessary if geolocations had zero latency ("prompt" case) – this implies that TGRS detects most bubbles repeatedly
- However, persistence is needed to help mitigate effective coverage loss due to realistic data latency

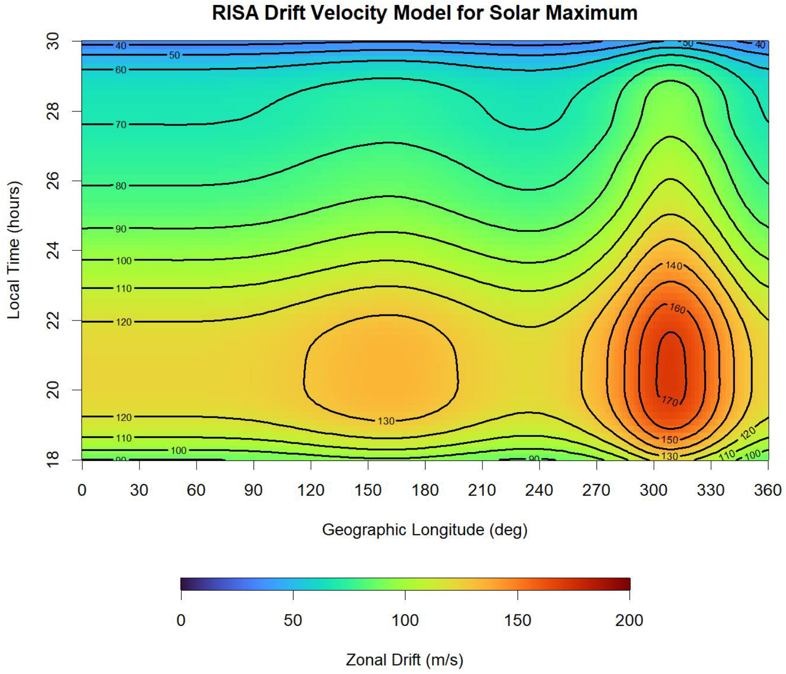

TGRS HR Data Latency

- Histograms & cumulative distributions for GPS & GLONASS HR data are shown below
- The impact of data latency on the Bubble Maps was assessed using scnPhs file generation time stamp information provided by UCAR

GPS

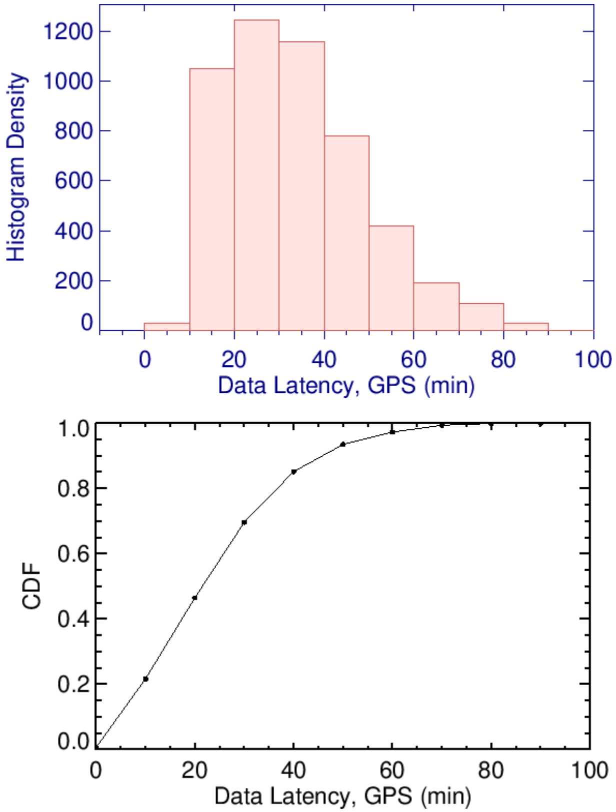

GLONASS

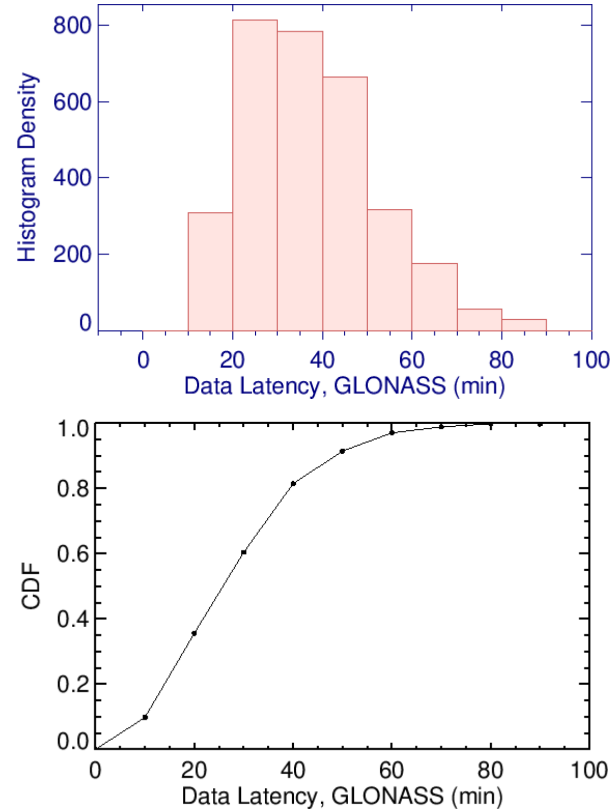

Prompt Data

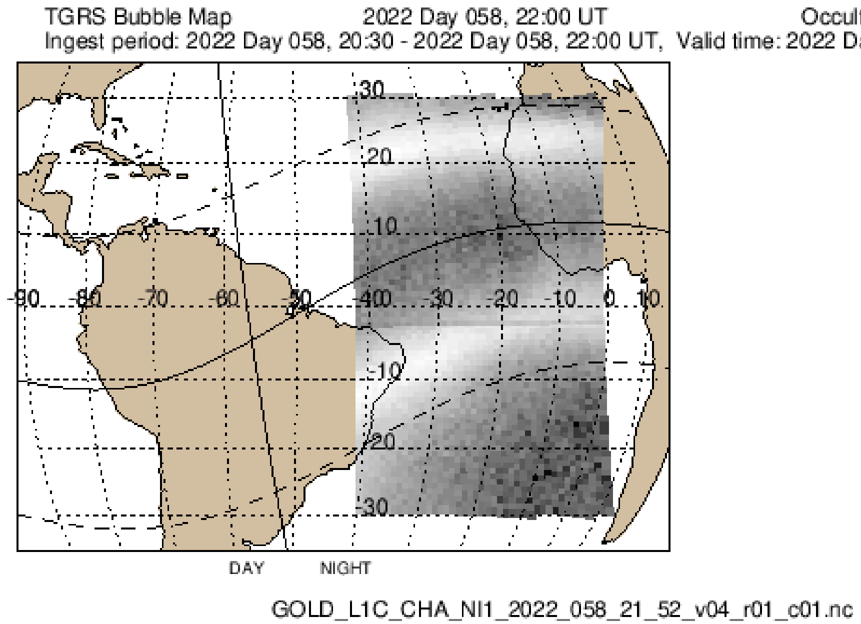

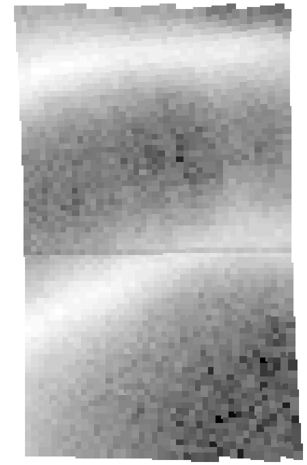

With Simulated Latency

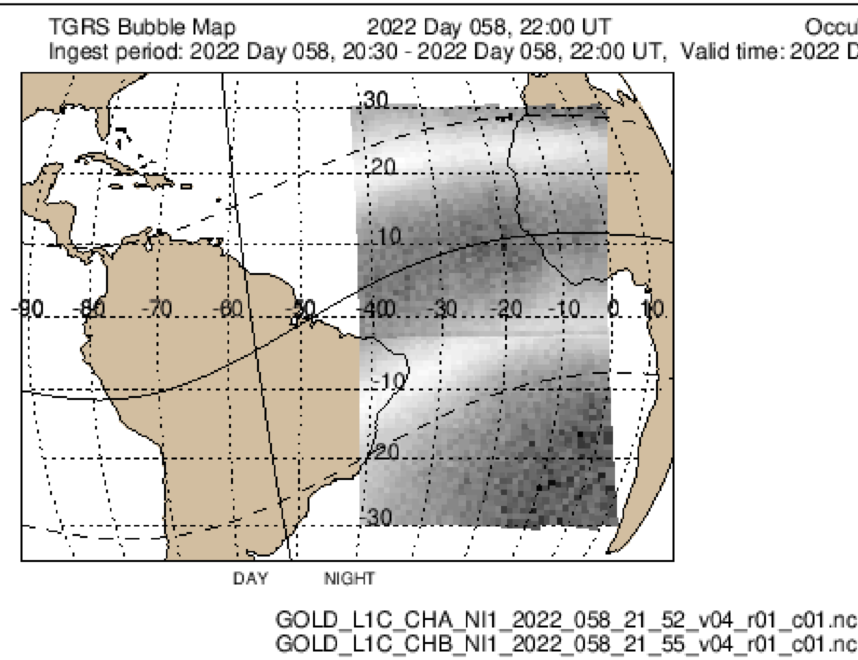

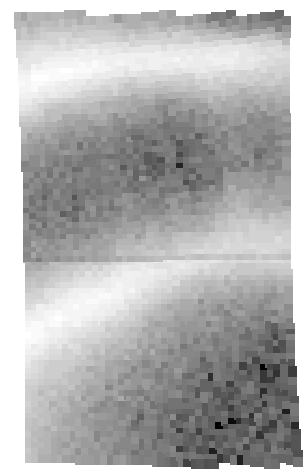

GOLD data is used to determine the effective “coverage” that the Bubble Maps provide

BC Analysis

Prompt Data

TGRS Bubble Map 2022 Day 058, 22:15 UT Occultations: 2, GEOs: 13
Ingest period: 2022 Day 058, 20:45 - 2022 Day 058, 22:15 UT, Valid time: 2022 Day 058, 22:15 UT

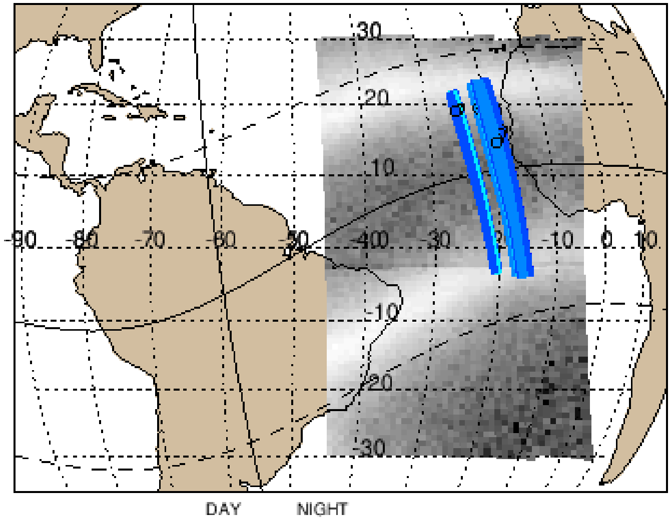

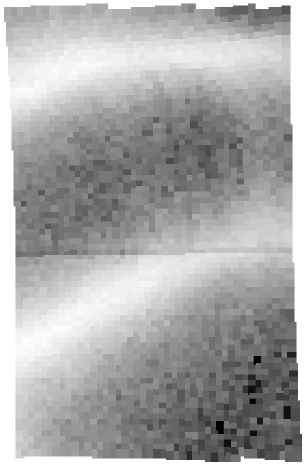

GOLD_L1C_CHA_NI1_2022_058_22_10_v04_r01_c01.nc

With Simulated Latency

TGRS Bubble Map 2022 Day 058, 22:15 UT Occultations: 0, GEOs: 0
Ingest period: 2022 Day 058, 20:45 - 2022 Day 058, 22:15 UT, Valid time: 2022 Day 058, 22:15 UT

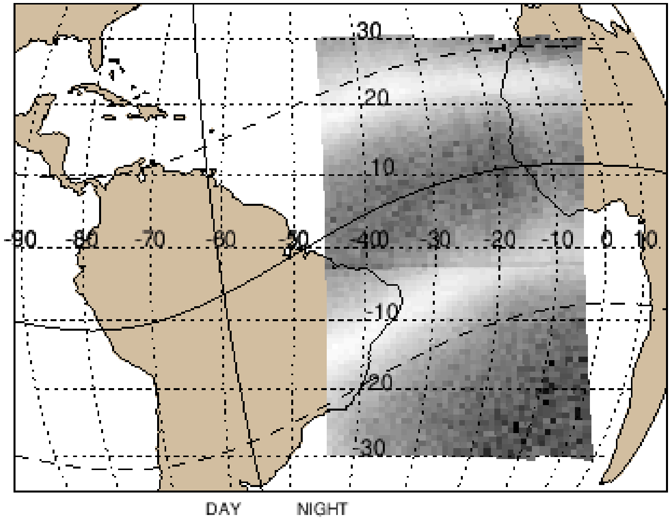

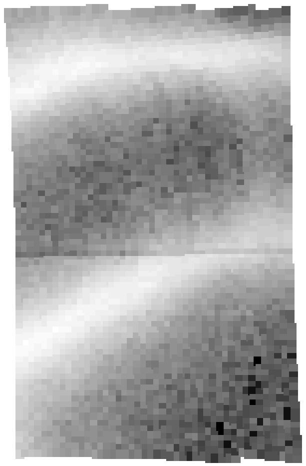

GOLD_L1C_CHA_NI1_2022_058_22_10_v04_r01_c01.nc
GOLD_L1C_CHB_NI1_2022_058_22_10_v04_r01_c01.nc

0.0 0.4 0.9 1.3 1.8 2.2 2.6
Log_{10}(Counts)

BC Analysis

Prompt Data

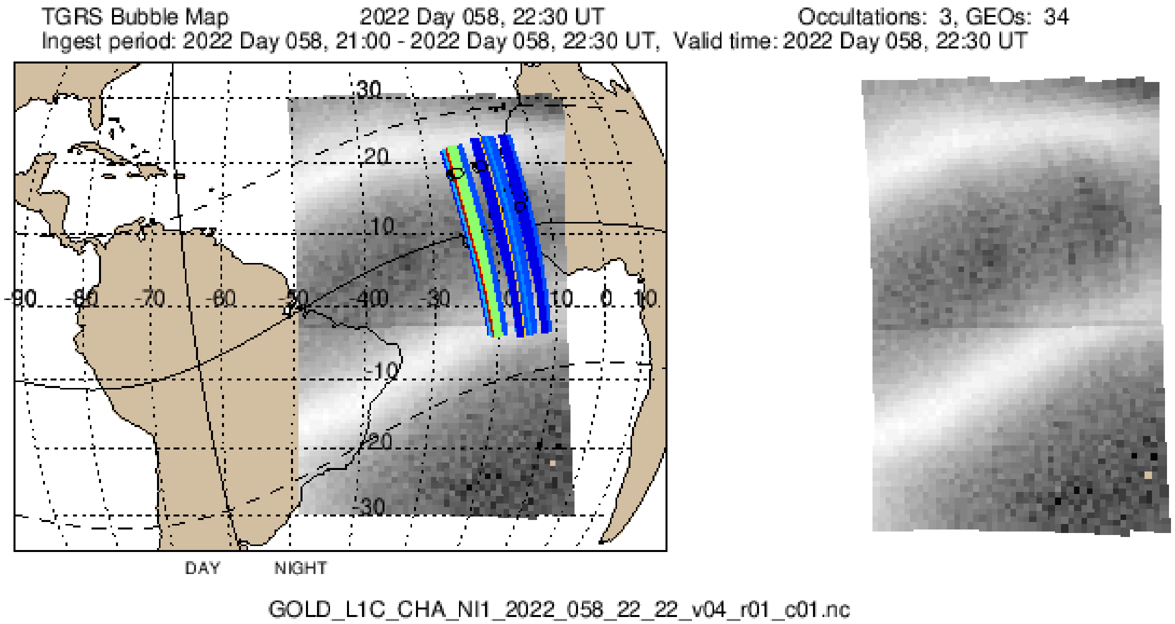

With Simulated Latency

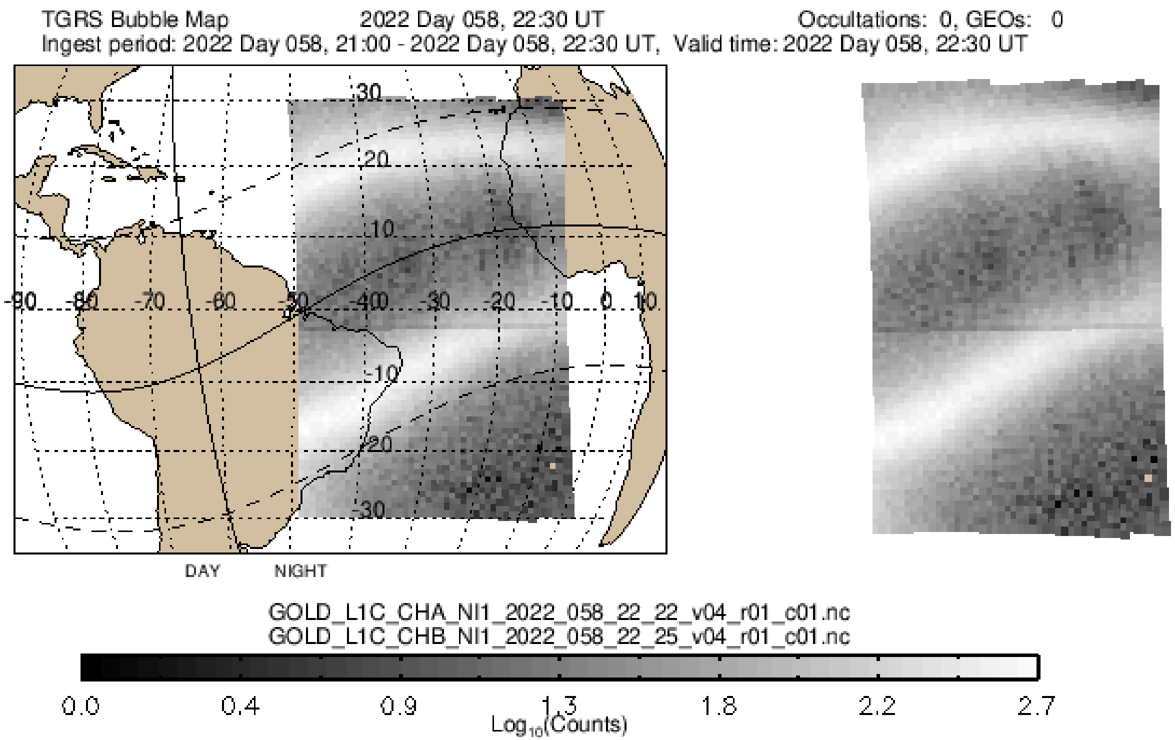

BC Analysis

Prompt Data

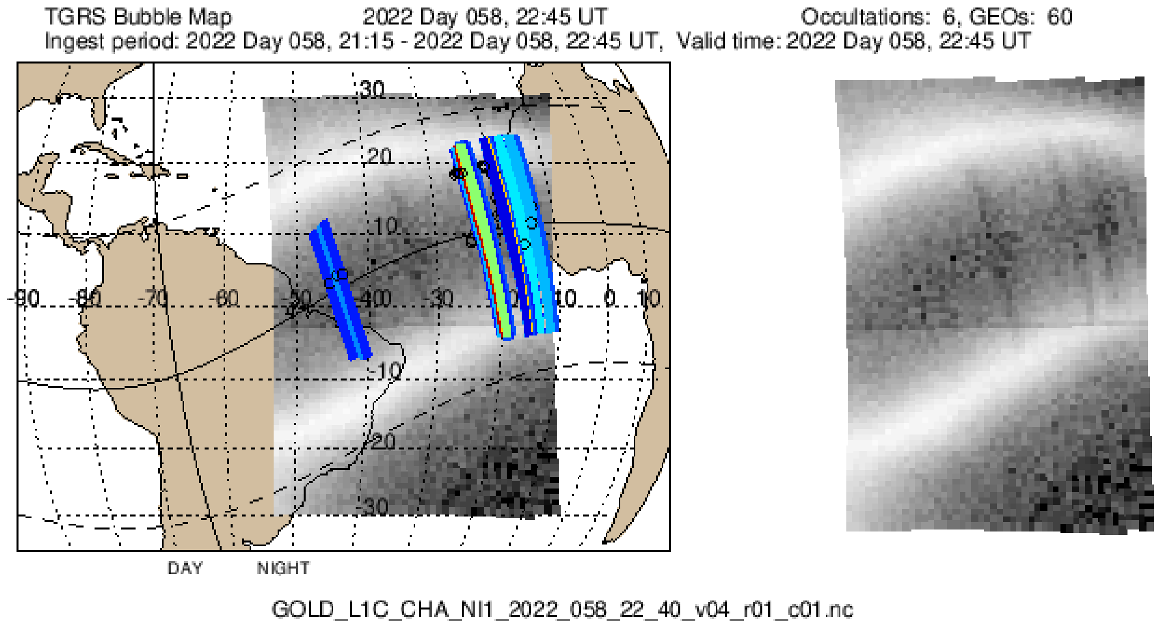

With Simulated Latency

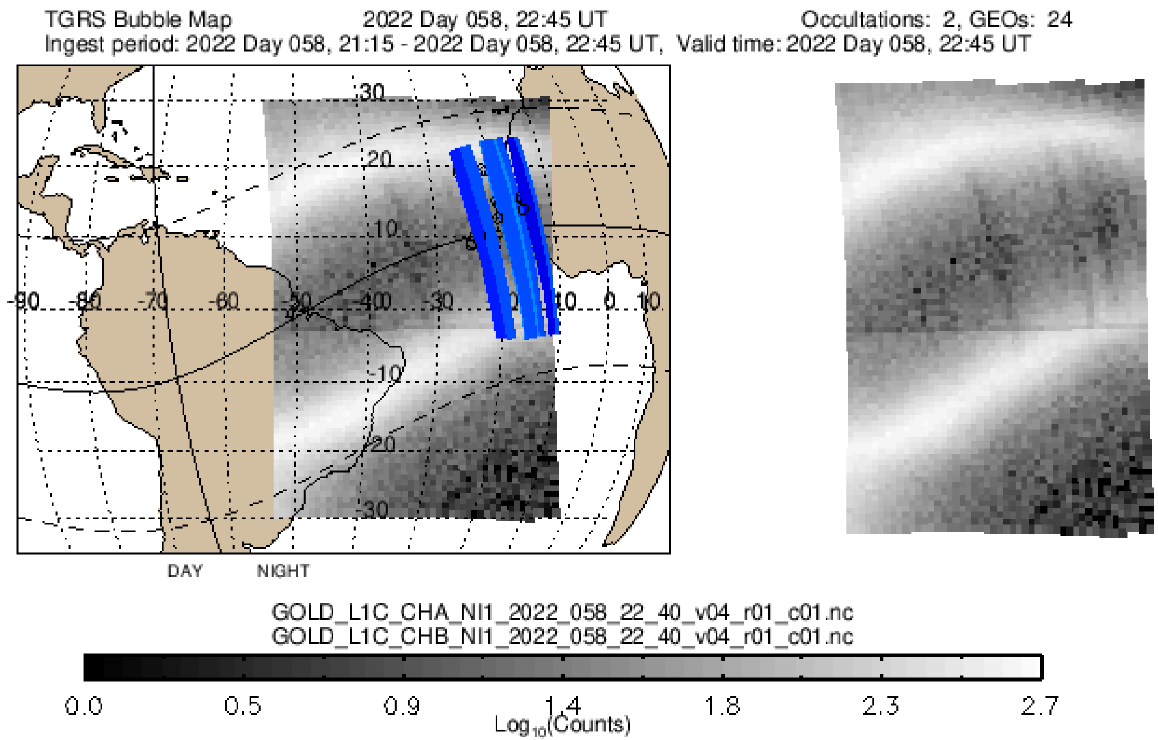

BC Analysis

Prompt Data

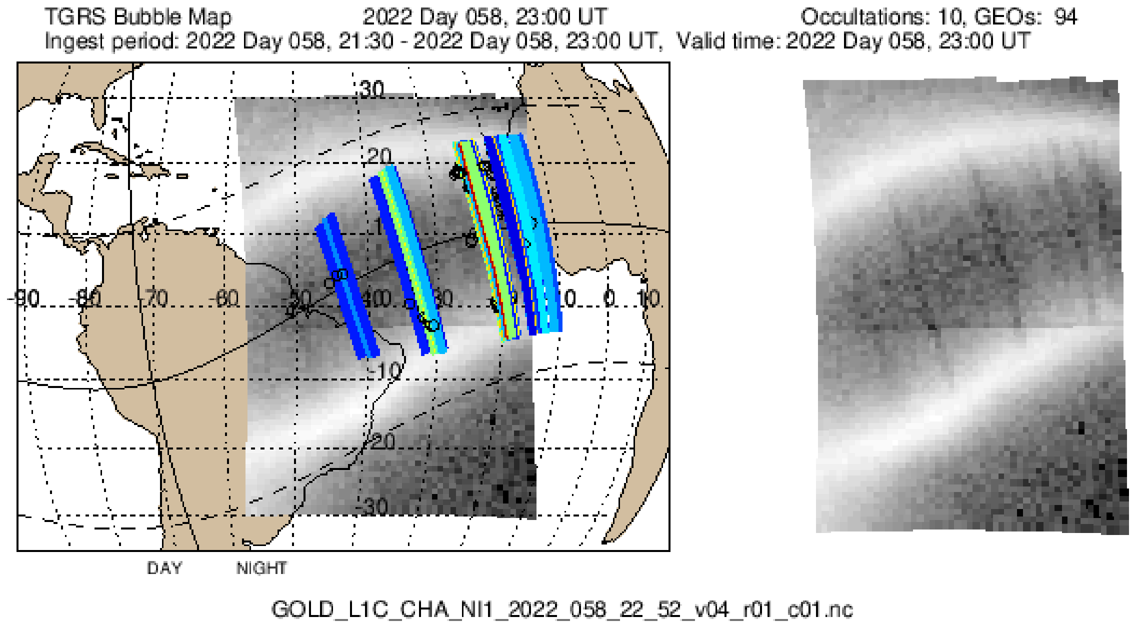

With Simulated Latency

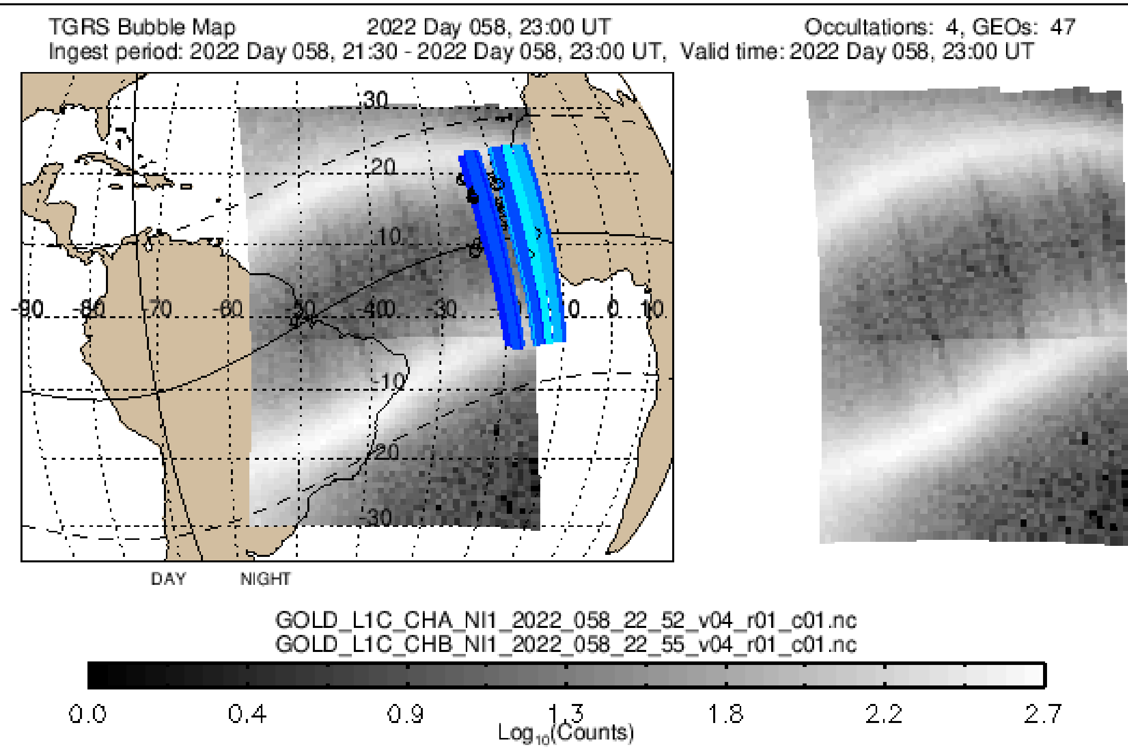

BC Analysis

Prompt Data

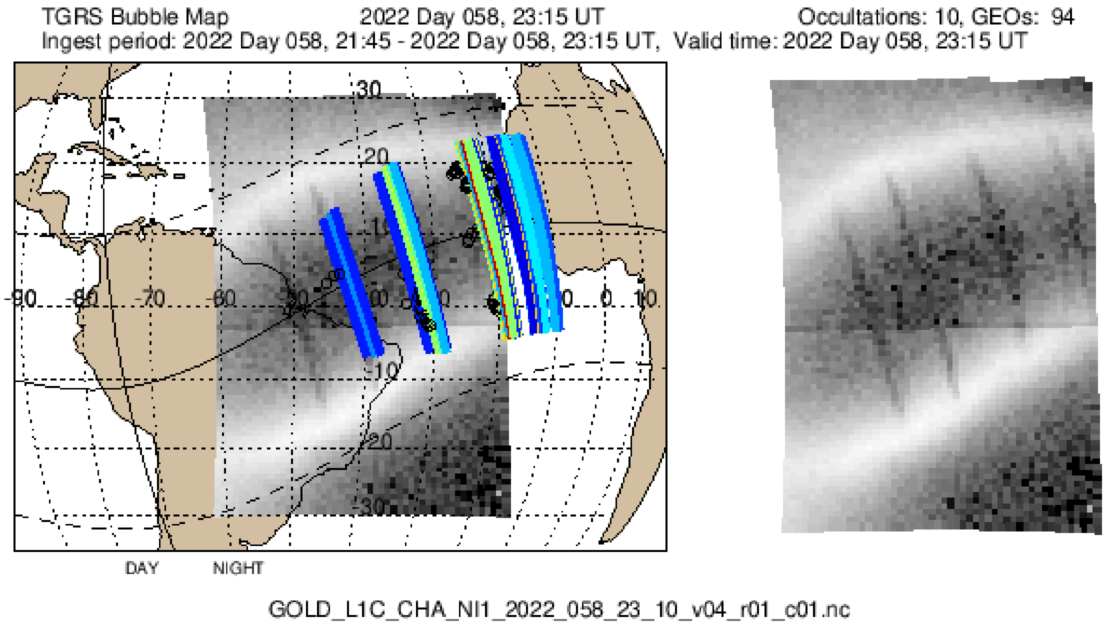

With Simulated Latency

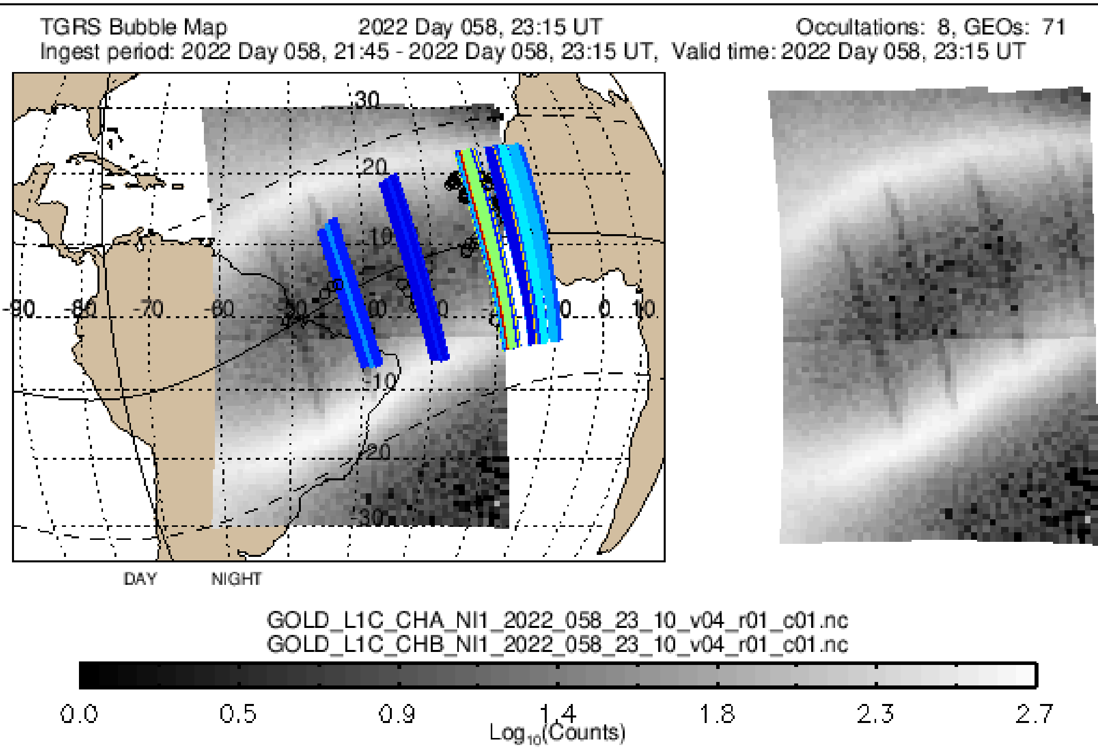

BC Analysis

Prompt Data

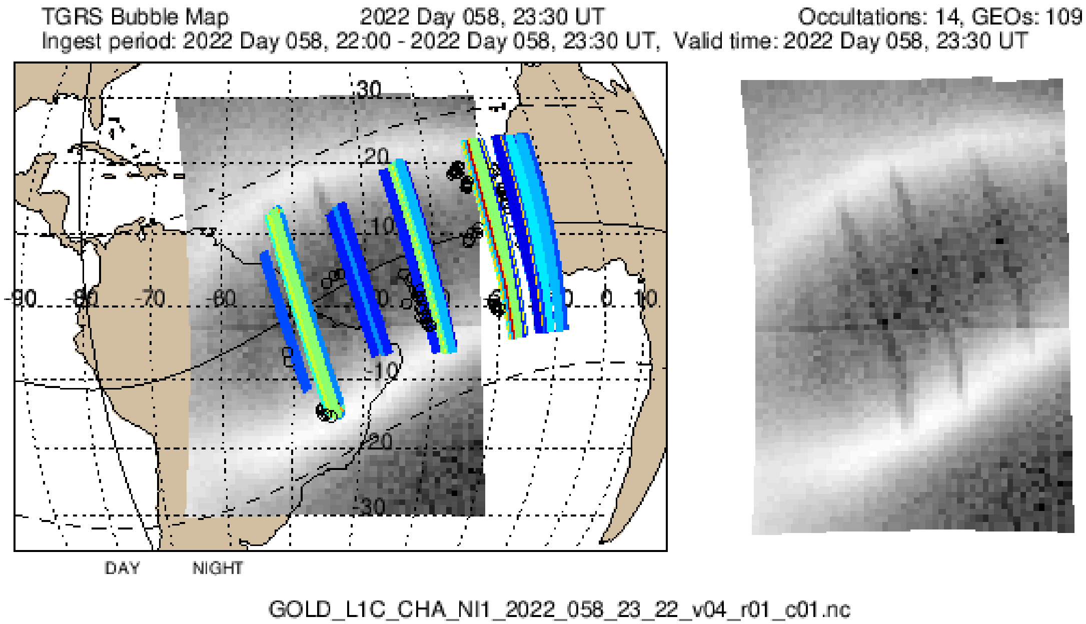

With Simulated Latency

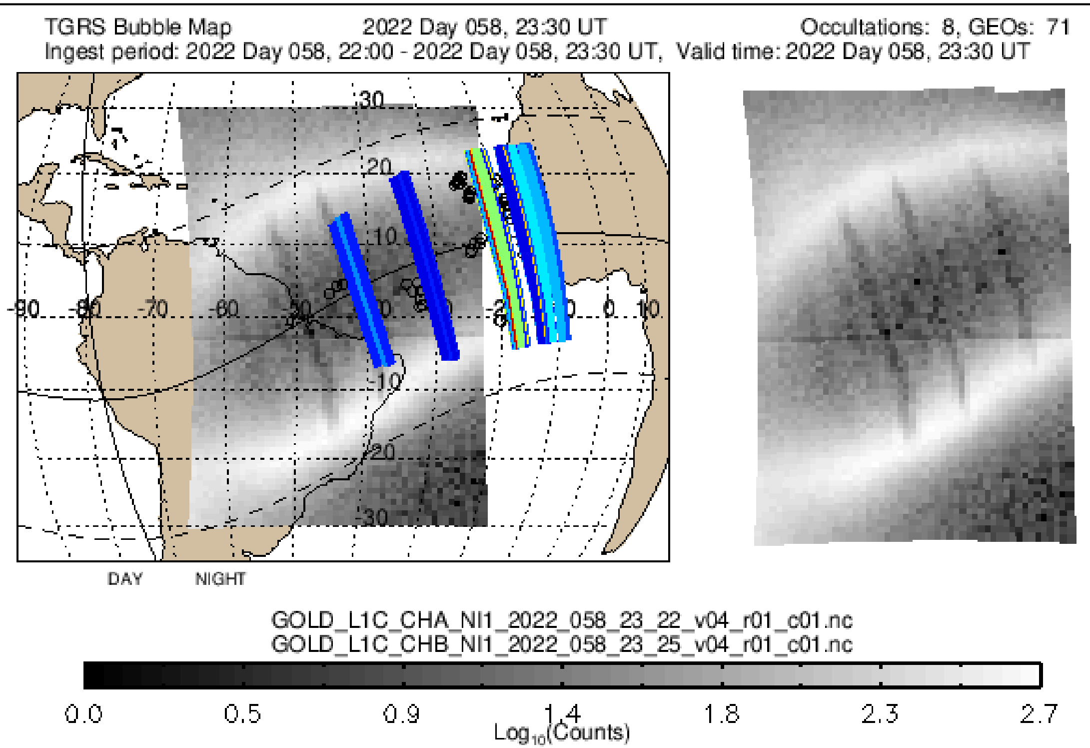

Prompt Data

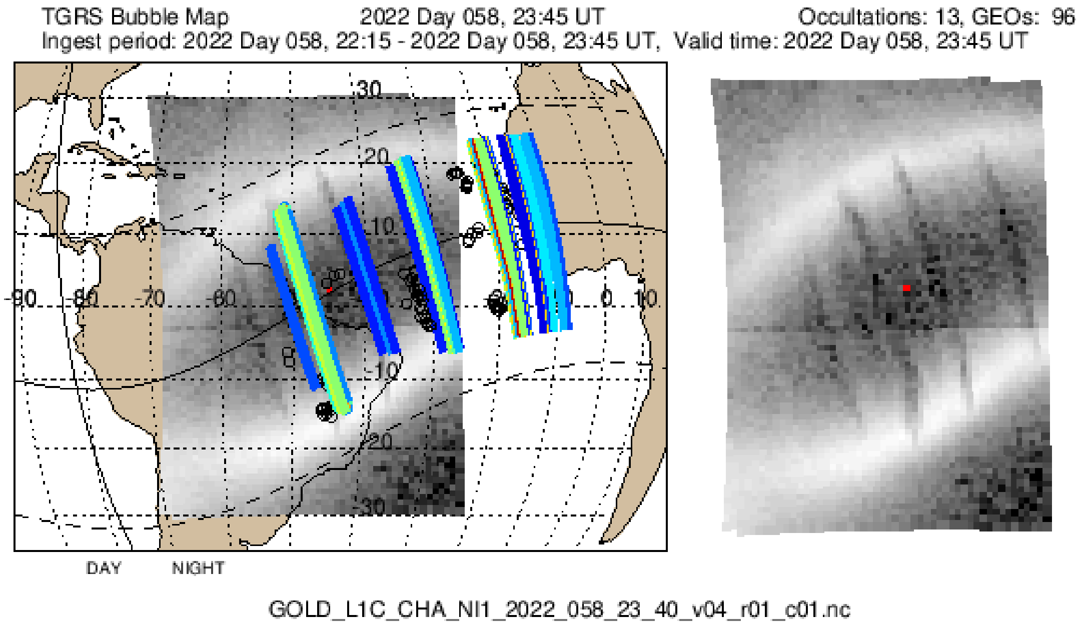

With Simulated Latency

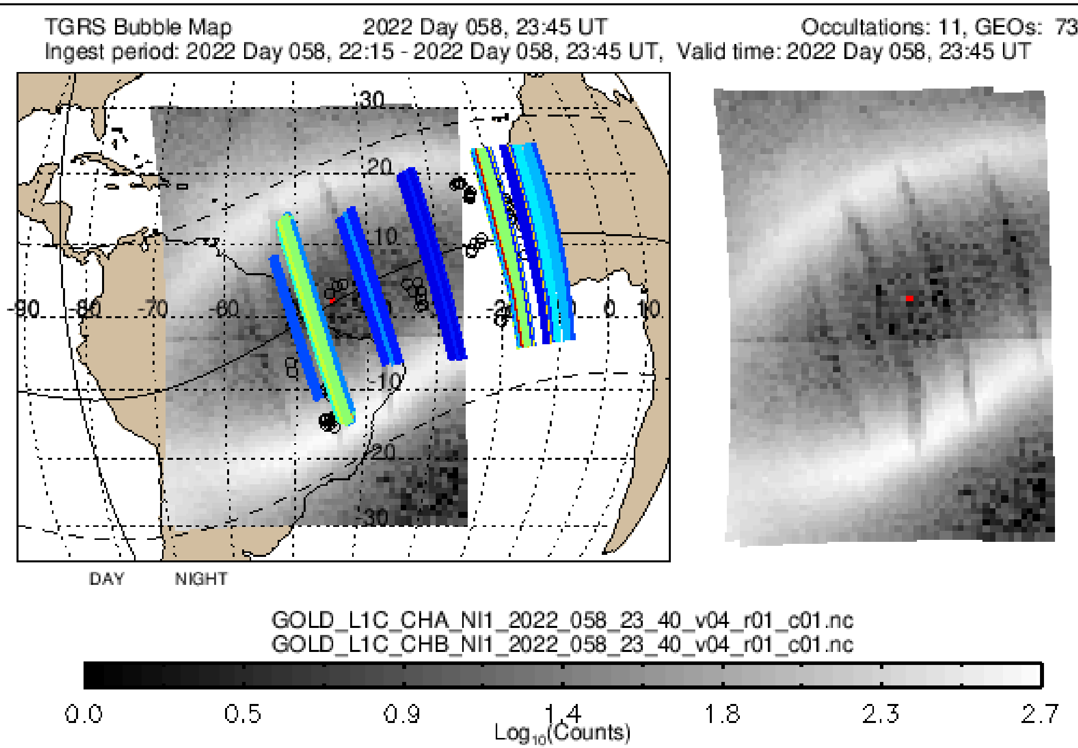

BC Analysis

Prompt Data

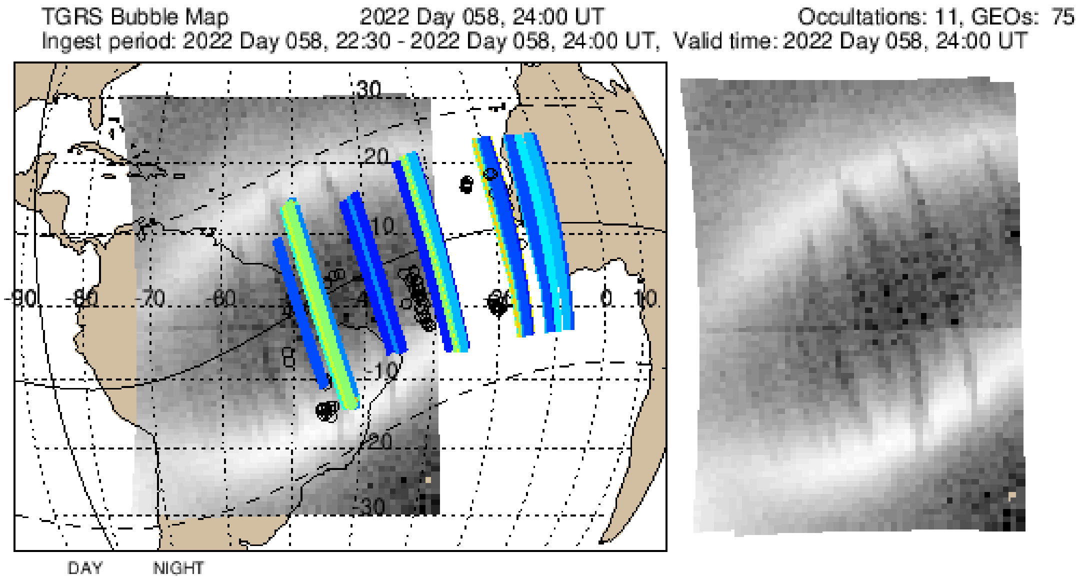

GOLD_L1C_CHA_NI1_2022_058_23_52_v04_r01_c01.nc

With Simulated Latency

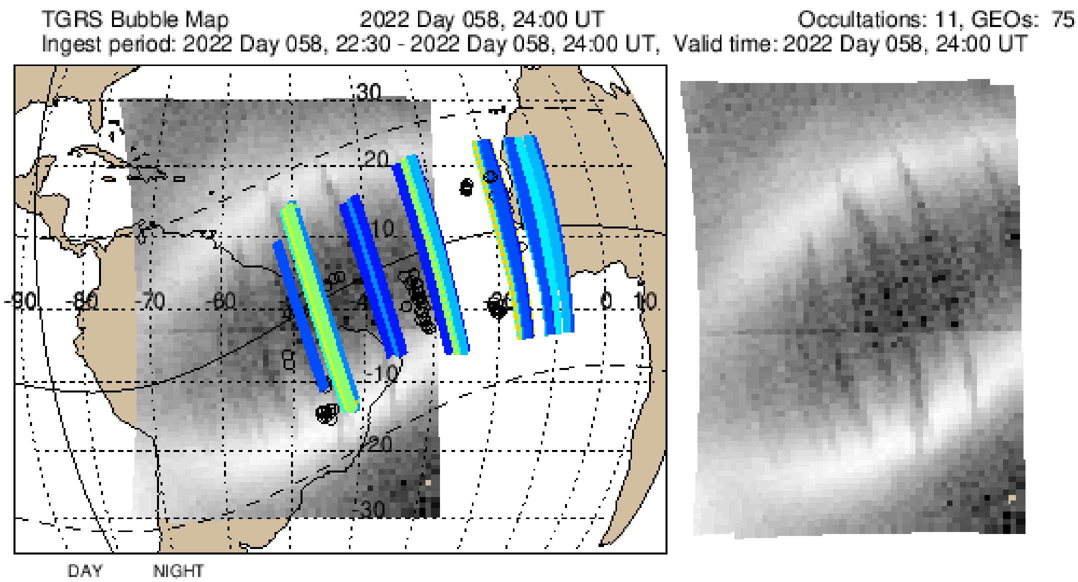

GOLD_L1C_CHA_NI1_2022_058_23_52_v04_r01_c01.nc
GOLD_L1C_CHB_NI1_2022_058_23_55_v04_r01_c01.nc

BC Analysis

Prompt Data

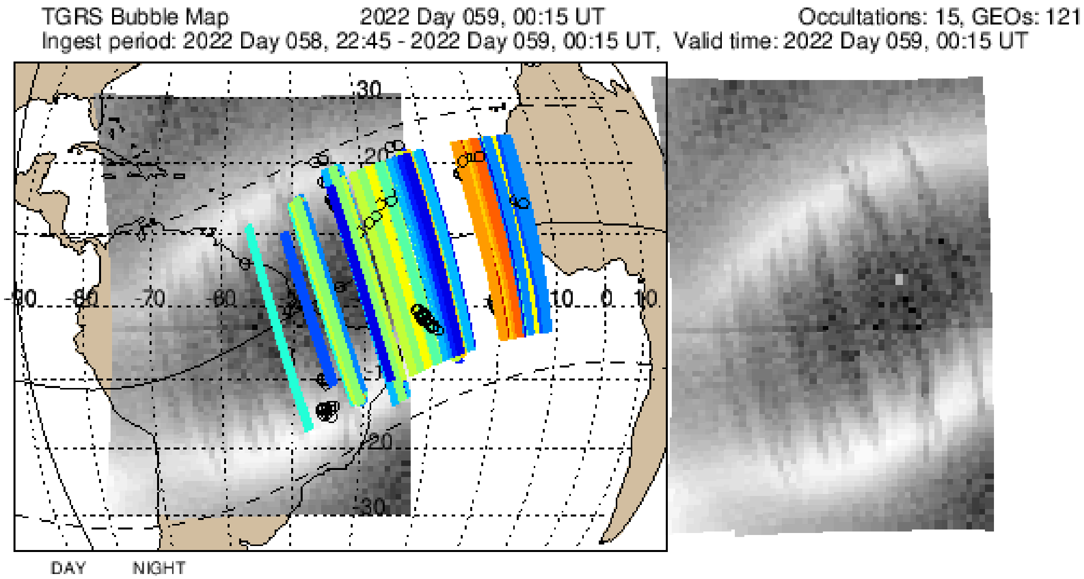

With Simulated Latency

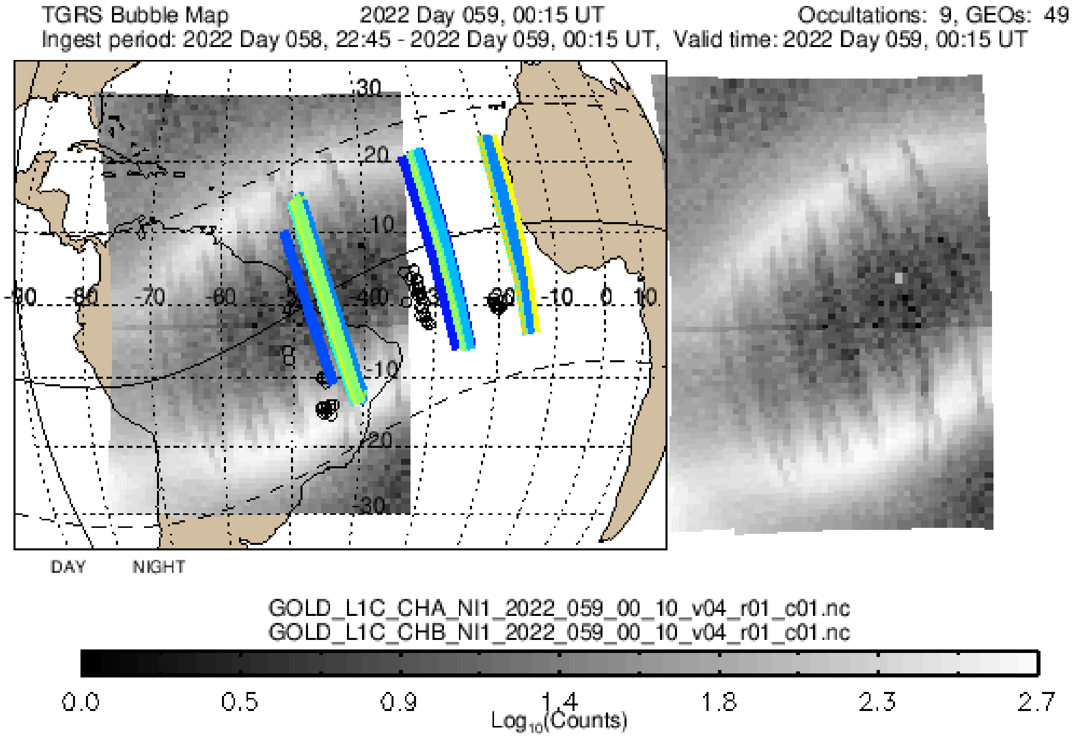

BC Analysis

Prompt Data

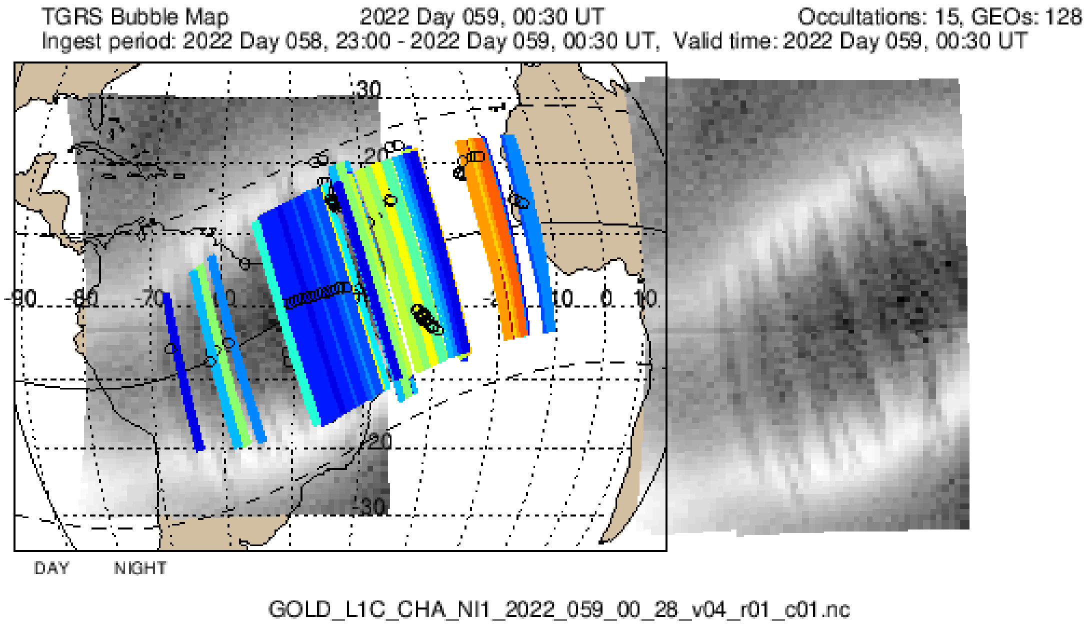

With Simulated Latency

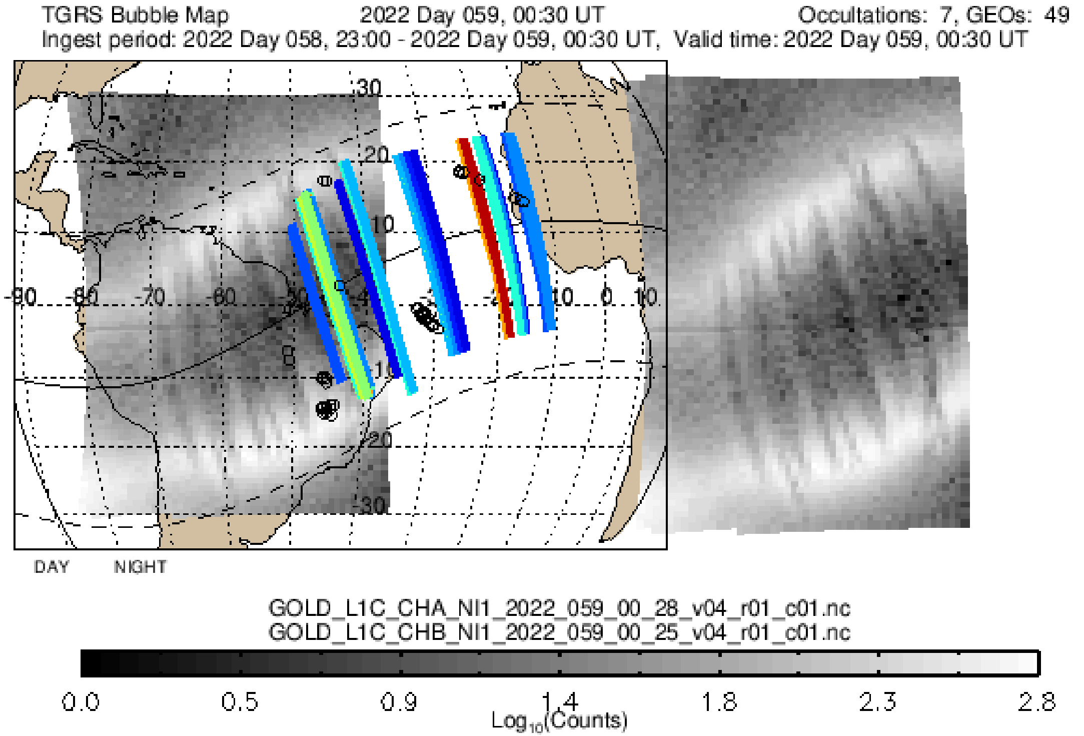

Bubble Map Effective Coverage

- The cumulative distribution function below summarizes effective Bubble Map coverage for "prompt" and realistic latency with different bubble persistence
- On average, 80% bubble coverage (relative to GOLD) is obtained 90% of the time in the prompt (unrealistic) case, but only 50% of the time with latent data
- The large separation between the prompt (solid) and latent (dashed) curves demonstrates the performance gap driven by data latency
- The lesser separation within each group of curves depicts differences due to persistence
  - *There is a clear advantage to using at least 90 minutes persistence in the case of realistic latency*

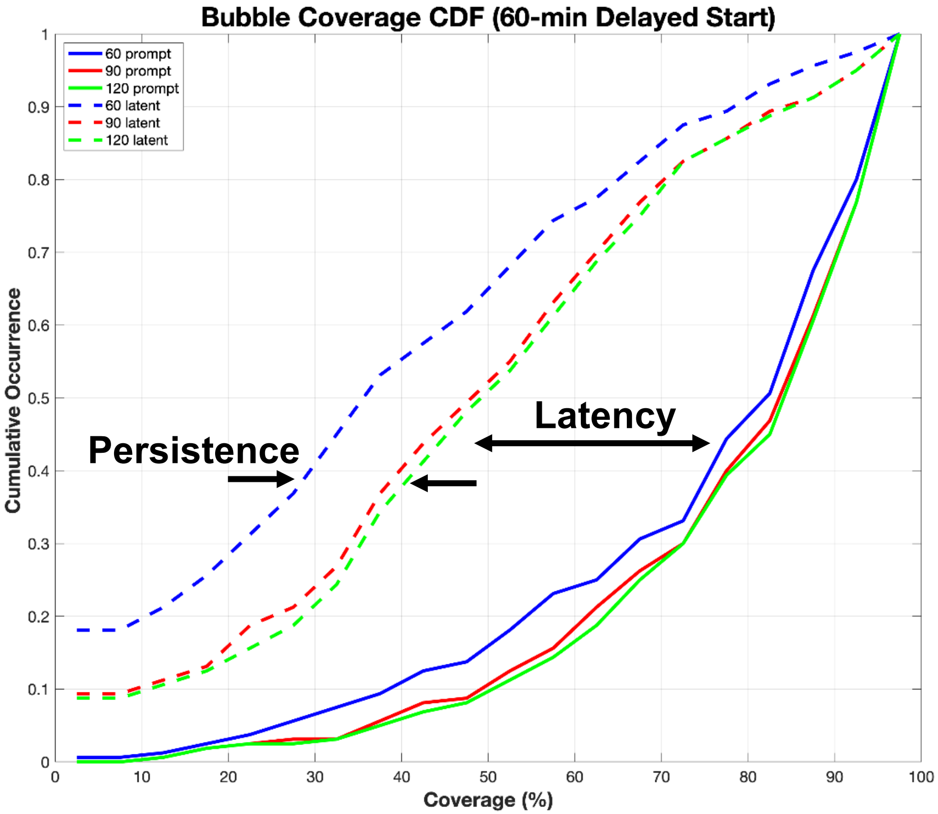

IVM-Based Bubble Map Development

Algorithm developed by UCAR

In-situ density data → Calculation/thresholding of Bubble Presence & Depth Indices → Mapping along orbit tracks → Bubble extension within equatorial region

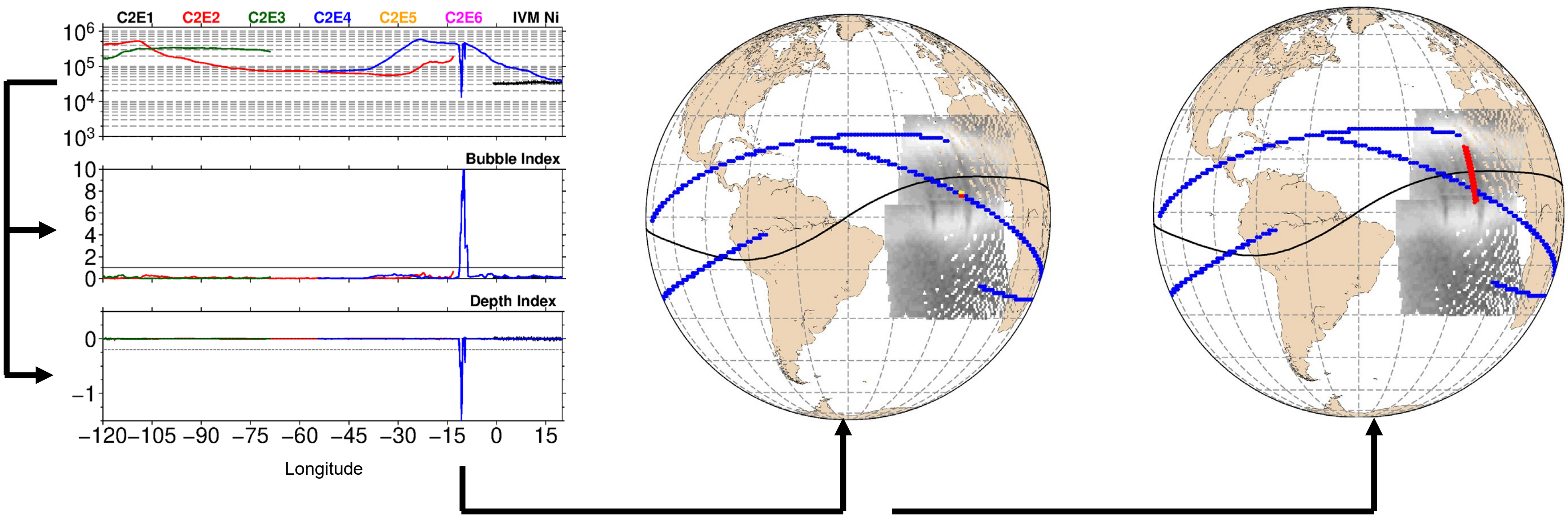

IVM in-situ density data can also be used to detect plasma bubbles

Comparisons to GOLD & Path Forward

- Initial analysis is promising, but much additional work remains:
- Assessment of the degree to which bubbles rise up high enough to be seen by IVM
- Can we tell the difference between “live” and “dead” bubbles?
- Tuning of index thresholds to optimize map
- Validation of IVM Bubble Maps
- How to optimally combine TGRS and IVM maps to improve effective coverage/refresh

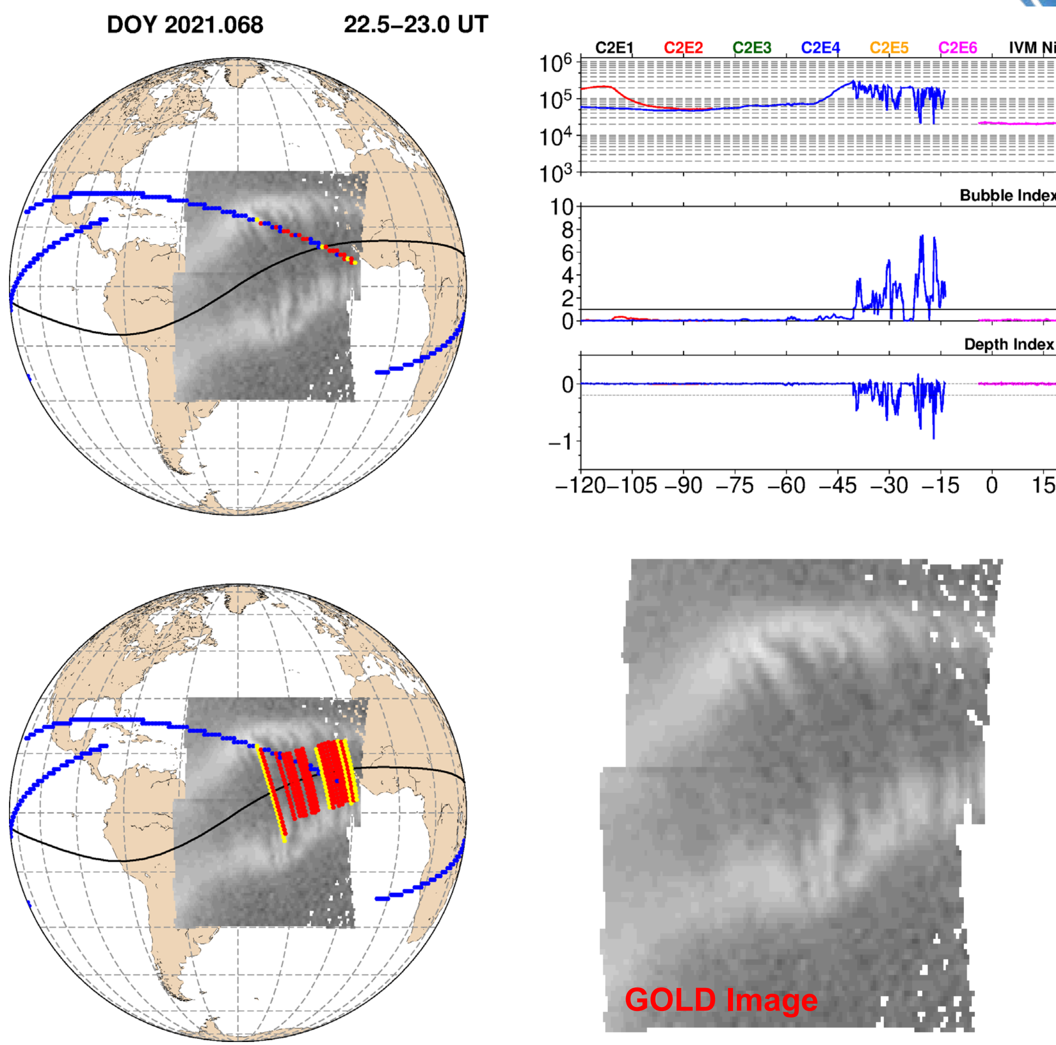

Considerations for Future RO Systems

Monitoring equatorial ionospheric scintillation

- COSMIC-2's low inclination orbits are optimal for scintillation monitoring
  - *High inclination orbits spend significant time at higher latitudes where they do not contribute to equatorial scintillation monitoring*
  - *Scintillation bubbles are better sensed by low inclination orbits that traverse north-south aligned bubbles each orbit – high inclination orbits can pass between bubbles*
- High-rate data at ionospheric tangent altitudes must be collected to enable accurate geolocation
- Low data latency is critical
  - *While excellent compared to most prior missions, COSMIC-2's 30min median latency is not sufficient to provide a complete map of scintillation activity on ionospheric instability development time scales*

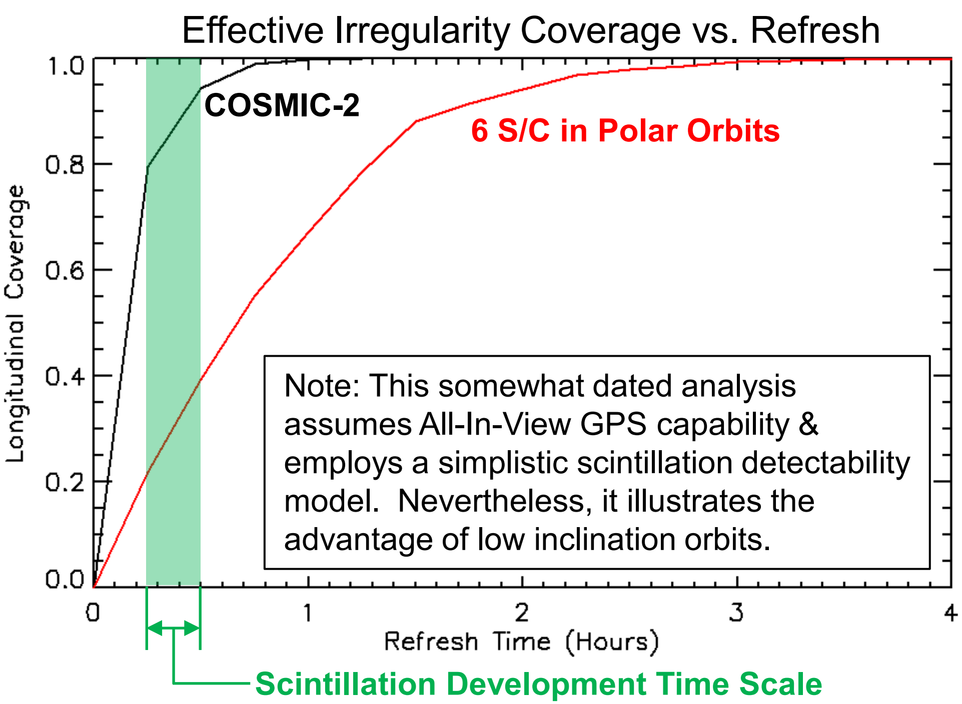

Summary

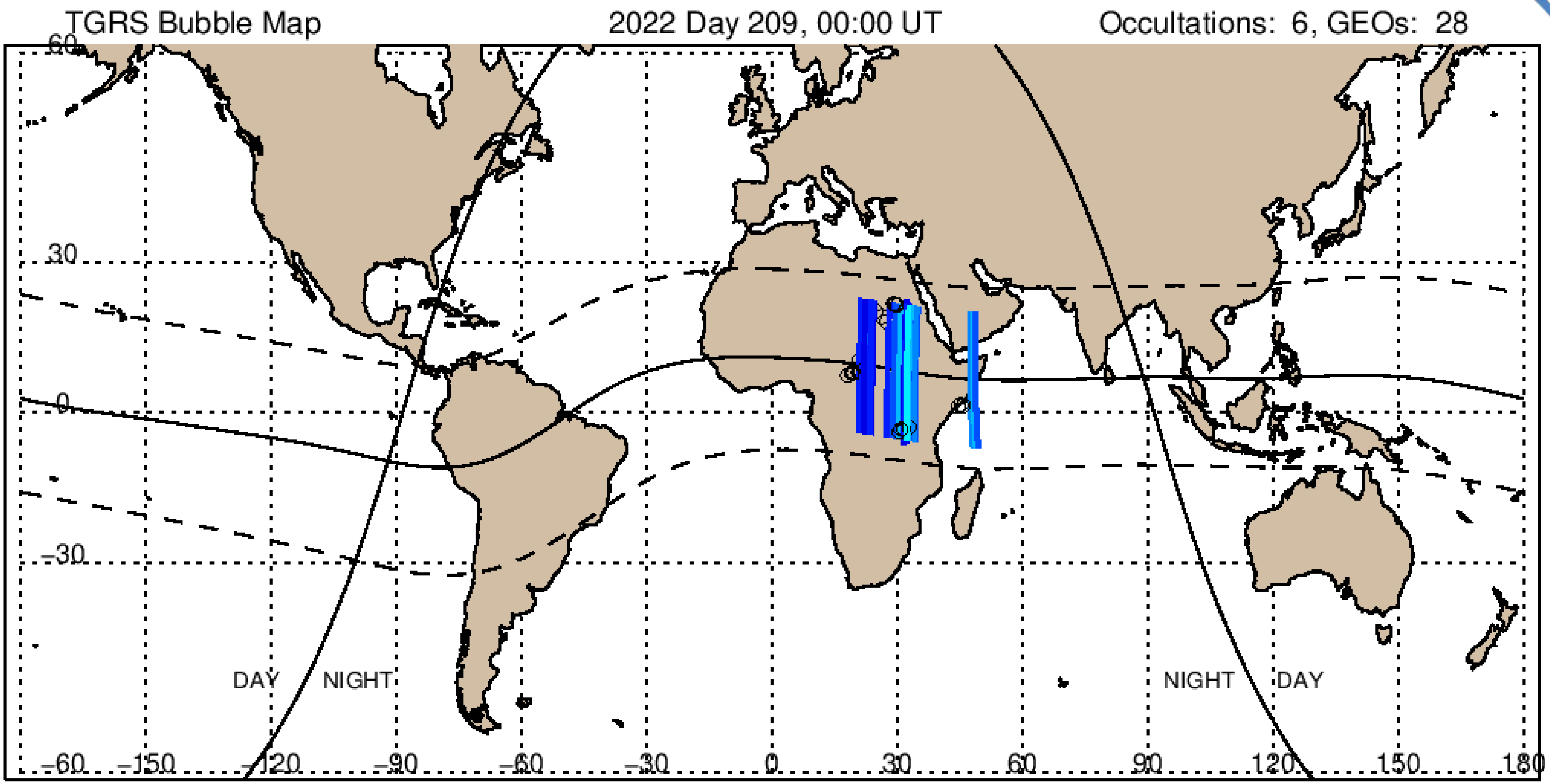

Advances in RO techniques for scintillation detection within the COSMIC-2 mission are providing science & operational communities with an unprecedented ability to monitor equatorial ionospheric scintillation